FORCED CONVECTION HEAT TRANSFER FROM A HEATED PIPE IN A TANK

2022
MASTER THESIS
MECHANICAL ENGINEERING

Ibrahim Amer MAHMOOD

Thesis Advisor
Assist. Prof. Dr. Abdulrazzak AKROOT

FORCED CONVECTION HEAT TRANSFER FROM A HEATED PIPE IN A TANK

Ibrahim Amer MAHMOOD

T.C.
Karabük University
Institute of Graduate Programs
Department of Mechanical Engineering
Prepared as
Master Thesis

Thesis Advisor
Assist. Prof. Dr. Abdulrazzak AKROOT

KARABÜK
November 2022

I certify that in my opinion, the thesis submitted by Ibrahim Amer Mahmood titled "FORCED CONVECTION HEAT TRANSFER FROM A HEATED PIPE IN A TANK" is fully adequate in scope and in quality as a thesis for the degree of Master of Science.

Assist. Prof. Dr. Abdulrazzak AKROOT .....
Thesis Advisor, Department of Mechanical Engineering

This thesis is accepted by the examining committee with a unanimous vote in the Department of Mechanical Engineering as a Master of Science thesis.

Examining Committee Members (Institutions)	Signature
Chairman : Prof. Dr.Kamil ARSLAN (KBU)	.....
Member: Assoc. Prof. MUNIR ELFARRA (YBU)	.....
Member: Assist. Prof. Dr. Abdulrazzak AKROOT (KBU)	.....

The degree of Master of Science by the thesis submitted is approved by the Administrative Board of the Institute of Graduate Programs, Karabuk University.

Assoc. Prof. Dr. Müslüm KUZU .....
Director of the Institute of Graduate Programs

This thesis contains information that I have gathered and presented in a manner that is consistent with academic regulations and ethical principles, and I affirm that I have appropriately cited any and all sources that are not my own work.

Ibrahim Amer MAHMOOD

ABSTRACT

M. Sc. Thesis

FORCED CONVECTION HEAT TRANSFER FROM A HEATED PIPE IN A TANK

Ibrahim Amer MAHMOOD

Karabük University
Institute of Graduate Programs
The Department of Mechanical Engineering

Thesis Advisor:

Assist. Prof. Dr. Abdulrazzak AKROOT

November 2022, 61 pages

In forced convective heat transfer, an outside force, such as a fan or pump, causes fluid or air to move. The heat transmission rate is higher with forced convection than with natural convection. This study contributed to discovering the effect of water flow on the rate of heat transfer from a cylinder placed in the middle of several cylinders similar to it and comparing its results with the side cylinders in order to determine which cylinder has the higher rate of heat transfer. Moreover, this study is very rare because the liquid flow in it is parallel to the hot cylinders when using forced convection heat transfer. In this experiment, the effect of different heat fluxes on the transfer of heat via forced convection was investigated using three heated cylinders as part of a nine-cylinder assembly submerged in water. Three of the cylinders had resistance while the remaining six were made of aluminum and were empty. Heat Flux values and flow rates were modified and during the testing, the heat flux values were held at 14.75 W/m^2, 206.417 W/m^2, 663.482 W/m^2, 1,179.52347 W/m^2, 1,990.44586 W/m^2, 2,830.85633 W/m^2, 3,818.71 W/m^2, and 4,953.99858 W/m^2. However, the first value (14.75 W/m^2) was minimal, so it was

ignored. Three liquid flow rates, of 32.5 L/M, 25 L/M and 15.6 L/M, were used. A substantial L/D ratio of 45 cm was utilized to apply the heat flux uniformly. In this experimental examination, Reynolds numbers over the range $154.34 \leq Re_D \leq 212.51$ was used. The most important discovery in this study was that the surface temperature of the heated cylinders was higher in forced convection than in natural convection because there is water flow in forced convection. The effect of the water on the heat transfer rate from the surface of the heated cylinders decreases when the water flow velocity is raised. The results also showed that the water flow rate increases and the water temperature decreases while the surface temperature of the heated cylinders increases. The findings also presented a direct relationship between the dimensionless numbers and the fluid flow rate. The side-heated cylinders lose more heat than the heated cylinder placed in the middle of the group because the side-heated cylinders affect the speed of water flow in the middle of the group and because there is also the chimney effect. The water on the surface is heated proportionally with an increasing axial length of up to 700 mm. At this point, it begins to decrease due to the turbulent mixing of cold and hot water flowing from the hot cylinders.

Keywords **:** Heat transfer, external forced convection, vertical long heated cylinders, flow across a tube bank.

Science Code : 91436

ÖZET

M. Sc. Thesis

TANK İÇERİSİNDEKİ ISITILMIŞ BİR BORUDAN ZORLU KONVEKSİYONLU ISI AKTARIMI

Ibrahim Amer MAHMOOD

Karabük Üniversitesi
Lisansüstü Eğitim Enstitüsü
Makine Mühendisliği Anabilim Dalı

Tez Danışmanı:

Dr. Öğr. Üyesi Abdulrazzak AKROOT

Kasım 2022, 61 sayfa

Zorlanmış konvektif ısı transferinde, fan veya pompa gibi bir dış kuvvet sıvı veya havanın hareket etmesine neden olur. Zorlanmış konveksiyonda ısı iletim hızı, doğal konveksiyona göre daha yüksektir. Bu çalışma, kendisine benzer birkaç silindirin ortasına yerleştirilmiş bir silindirden su akışının ısı transfer hızı üzerindeki etkisinin keşfedilmesine ve sonuçlarının yan silindirlerle karşılaştırılarak hangi silindirin daha yüksek ısı transfer hızına sahip olduğunu belirlemeye katkıda bulunmuştur. . Ayrıca, zorlanmış konveksiyon ısı transferi kullanıldığında içindeki sıvı akışı sıcak silindirlere paralel olduğu için bu çalışma çok nadirdir. Bu deneyde, farklı ısı akılarının zorlanmış konveksiyon yoluyla ısı transferi üzerindeki etkisi, suya daldırılmış dokuz silindirli bir düzeneğin parçası olarak üç ısıtmalı silindir kullanılarak araştırıldı. Silindirlerden üçü dirençliyken, geri kalan altısı alüminyumdan yapılmış ve boştu. Isı Akısı değerleri ve akış hızları değiştirildi ve test sırasında ısı akısı değerleri 14,75 W/m2, 206,417 W/m2, 663,482 W/m2, 1.179,52347 W/m2, 1.990.44586 W/m2, 2.830.85633 W/m2, 3.818,71 W/m2 ve

4.953,99858 W/m2. Ancak ilk değer (14,75 W/m2) minimum olduğu için dikkate alınmadı. 32,5 L/M, 25 L/M ve 15,6 L/M'lik üç sıvı akış oranı kullanıldı. Isı akışını eşit şekilde uygulamak için 45 cm'lik önemli bir L/D oranı kullanıldı. Bu deneysel incelemede $154.34 \leq ReD \leq 212.51$ aralığındaki Reynolds sayıları kullanılmıştır. Bu çalışmadaki en önemli keşif, ısıtılmış silindirlerin yüzey sıcaklığının zorunlu taşınımda su akışı olduğu için doğal taşınıma göre daha yüksek olmasıdır. Suyun ısıtılan silindirlerin yüzeyinden ısı transfer hızı üzerindeki etkisi, su akış hızı arttıkça azalır. Sonuçlar ayrıca ısıtılan silindirlerin yüzey sıcaklığı artarken su debisinin arttığını ve su sıcaklığının düştüğünü göstermiştir. Bulgular ayrıca boyutsuz sayılar ile sıvı akış hızı arasında doğrudan bir ilişki olduğunu ortaya koydu. Yandan ısıtmalı silindirler grubun ortasına yerleştirilen ısıtmalı silindire göre daha fazla ısı kaybeder çünkü yandan ısıtmalı silindirler grubun ortasındaki su akış hızını etkiler ve baca etkisi de vardır. Yüzeydeki su, 700 mm'ye kadar artan bir eksen uzunluğu ile orantılı olarak ısıtılır. Bu noktada sıcak silindirlerden akan soğuk ve sıcak suyun türbülanslı karışımından dolayı azalmaya başlar.

Anahtar Kelimeler : Isı transferi, harici zorlanmış konveksiyon, dikey uzun ısıtmalı silindirler, bir tüp kümesi boyunca akış.

Bilim Kodu **:** 91436

ACKNOWLEDGEMENT

The first to whom to give thanks and praise during the night and the end of the day is the Highest, the Kahar, the First and the Last, the Apparent and the Inward, Who showers us with his countless blessings, blesses us with His endless provision, and illuminates our paths. Upon us, when He sent among us His servant and Messenger, Muhammad bin Abdullah, may God's prayers and peace be upon Him and His family, He sent him with his clear Qur'an, so He taught us what we did not know and urged us to seek knowledge wherever it was found. All praise and thanks are due to God for granting us success and inspiring us with patience and the eagerness for that which confronts us to accomplish this humble work, and thanks go to every teacher who helped me with his knowledge, from the first stages of this study until this moment. I also extend a word of thanks to Assist. Prof. Dr. Abdulrazzak Akroot. I wish him all the best and much success. I also thank the Head of the Department of Mechanical Engineering, Prof. Dr. Kamil ARSLAN, and his staff for the assistance they have given me. My thanks and gratitude to Dr. Zaid Ali for his support. Thanks also go to my colleagues Mr. Zain, Nasir, Ibtisam, Shahd, Wissam, Aya, Hamza, Alyaa, Farah, Othman, Ahmed and all the others who had helped me to provide this achievement, wishing them the best ranks and success. I dedicate my achievement to my dear country, Iraq, and my city Baghdad, which is steadfast by its people, and to my second country Turkey, and to the man who taught me, supported me, and inspired me, my dear father, may God prolong his life, and to whom her satisfaction is my goal and purpose, to the one who gave me everything and who did not expect from me any kind word of thanks, to the motivator of my determination, without whom I am nothing, to the woman who made me from nothing, my beloved mother, may God prolong her life, to my family, my people, my brother, my sister, my uncle Maher and his family. Finally, I can only pray to God Almighty to grant us guidance, chastity, wealth, health, safety, and who inspires me with more determination and strength to upgrade my scientific thesis and study the PhD, Inshallah.

CONTENTS

Page

Page

Page

LIST OF FIGURES

Page

Page

LIST OF TABLES

Page

SYMBOLS AND ABBREVITIONS INDEX

SYMBOL

Kf	: Thermal conductivity by mean temperature
L	: Total heated length of the cylinder
Nu_D	: Average Nusselt number
$\mathrm{Nu}_{D,\ NL}$	: Average Nusselt number are for tube banks with 16 rows
N	: Number of heated cylinders
N_L	: The number of rows
N_T	: The number of columns
V	: Voltage
I	: Current
P	: Power
$\mathrm{Q}_{\mathrm{cond}}$	: Conduction heat transfer
Q_{conv}	: Convection heat transfer
$\mathrm{Q}_{\mathrm{rad}}$	: Radiation heat transfer
$q"$	: Heat flux (P/As)
Re_D	: Average Reynolds number
$\mathrm{T_m}$	: Mean temperature of water
T_i	: Temperature of water in the inlet
T_e	: Temperature of water in the outlet
T_{sav}	: Average temperature of cylinder surface
T_s	: Surface temperature of cylinder
$\Delta\mathrm{T}_{\mathrm{in}}$	: Logarithmic mean temperature difference
V	: Flow velocity
V_{max}	: Maximum velocity
h	: Heat transfer coefficient
D	: Diameter of cylinder
As	: The surface area of the heated cylinders

SYMBOL

$\dot{V}$: Volume flow rate

Q : Flow rate

S_T : The distance between the centers of two cylinders

Pr : Prandtl number by mean temperature

Pr_s : Prandtl number by Surface temperature

F : Correction factor

$\dot{W}_P$: Pumping power

ΔP : Pressure drop

Ƒ : Friction factor

χ : Correction factor

μ : Water viscosity by mean temperature

ρ : Water density by mean temperature

PART 1

INTRODUCTION

Heat is transferred either inside systems themselves or between the systems and their surroundings whenever there is a temperature differential between two different systems [1]. In relation to transporting thermal energy, one can select from a variety of diverse approaches. It is frequently possible to explore the various heat transmission techniques autonomously. Any data gathered can then be combined to calculate the overall quantity of heat transferred by the system. On the other hand, it is sometimes necessary to use various heat transfer strategies to remove heat from a system successfully. A wide range of businesses follows the forced convection method to enhance their operations. Given how frequently forced heat transfer by convection is employed in industrial settings, it is imperative to show how water velocity affects the coefficients for forced convection heat transfer. Readings of the temperature taken from the vertical plane of a heating material are required for the procedure to be considered complete. It has been investigated through experiments how heat is distributed through the use of forced convection. In the context of heat transmission, this is being done to investigate the connection between the Reynolds number and the Nusselt number [2]. Convective heat transfer coefficients have been shown to have a close relationship with one another. Additionally, currently available experimental data are compared.

The effects of forced convection are investigated using three thin cylinders stacked vertically. The fluid is forced to pass through and between these cylinders by a pressure differential, also sometimes referred to as an external push. The flow properties of a fluid significantly impact the convective process of moving heat through a fluid, also known as “convection.” Consequently, the transfer rate is influenced not only by the forced convective heat transfer but also by the speed at which the fluid is moving. Laminar or turbulent flow patterns can be used when determining the type of convective heat transfer that is occurring. This is so that both

of these flow patterns are indicative of different types of temperature transmission. It indicates that a forced convection system can transfer heat from fluctuations in fluid density that are produced by temperature changes in addition to transferring heat from external sources. The effects of forced convection are investigated using three thin cylinders arranged vertically. When a heat source is close to a cold fluid, the cold fluid can absorb heat from the heat source, which causes the fluid to rise. After this, heat travels from the surface of the liquid to the bottom of the convection cell. The liquid will be heated there before it is circulated back into the convection cell. The study of convective heat transfer is more difficult than conduction heat transfer [3] because no one attribute of the heat transfer fluid, such as thermal performance, can be recognized as the process. The conductivity of the fluid flow, which is typically related to the direction in which the flow occurs, affects the convective heat transmission. The removal of heat from spent nuclear fuel bundles, cooling nuclear reactor cores after an accident involving a loss of coolant, space shuttle launch pads, and stored spent nuclear rods are a few examples of applications in which forced convection from thin vertically heated cylinders present a significant challenge. Other examples also include the removal of heat through process pipes, methods applicable to coils, electric immersion heating in process vessels, the removal of heat from spent nuclear fuel bundles, and the cooling of nuclear reactor cores after an accident involving loss of containment. The following is merely a small sample of the wide variety of potential uses. Steam is used to heat coils. Heat is lost in the process pipes, and electric immersion heating is used in the process vessels.

There are only two variables that need to be taken into consideration, these being the Nusselt and Reynolds numbers for vertical isothermal surfaces. The flow type was laminar as the Reynolds values were [4]: $Re_D < 2{,}000$ laminar. The heat transfer that takes place on either side of a cylinder assembly is not the same as the heat transfer that takes place between a fluid that is placed surrounding a cylinder that is located in the center of an assembly of cylinders [5]. This is because the heat transfer on the side cylinders influences the cylinder placed in the middle of the vessel. In this experiment, the forced convection of a thin cylinder placed in the center and the

remainder positioned on its sides was studied experimentally using variable heat flux and different fluid flow rate values.

1.1. IDENTIFYING CONVECTION

Heat is transferred through convection, which is the extensive movement of molecules within gases and liquids [6]. Conduction is initially used to transfer heat from the object to the fluid, but fluid motion is ultimately responsible for most of the heat transfer:

1. Convection is the process by which heat is transferred through fluids due to material motion.
2. It occurs in both gases and liquids.
3. It may be forced or it may be natural.
4. Bulk transfers of some of the fluids are necessary.

Thermal expansion occurs in a fluid when it is heated from below. The lower, hotter layers of the fluid have a lower density than the remaining layers. It is common knowledge that colder fluids have a higher density. Because of buoyancy, the portion of the fluid that is hotter and less dense rises, after which it is replaced by fluid that is colder and denser. When this component also heats and rises, it is replaced by the higher, colder layer, which causes the process to repeat itself. Convection is the process by which heat is transferred in such a manner.

There are four different forms of convection [7]:

1. Internal natural convection.
2. Internal forced convection.
3. External natural convection.
4. External forced convection.

1.1.1. Internal Natural Convection

Compared to their counterparts outside, the problems associated with natural convection inside have received less attention from researchers. This is a direct result of the preeminent significance of external flows in operational practice. The significance of free boundary layer fluxes has been highlighted by research in the fields of heat rejection, meteorology, and pollution, as well as by research examining the flow of fluids across hot surfaces in industrial and energy systems. In addition, the results obtained for external flows are frequently considered to be important, even in internal flow problems. This is especially the case in transient problems for short times and large enclosures, in which flows over enclosed surfaces may behave independently and therefore allow their analyses as external flow circumstances.

In most cases, the complexity of internal flow problems is significantly higher than that of outward flow problems. Regarding the latter, it is assumed that everything beyond the boundary layer is immobile and unaffected by the current. After that, any flow-independent conditions stated outside the zone can be derived from the circumstances already known in the ambient fluid medium. A boundary layer flow may exist near the walls during natural convection flows in enclosures. However, the region beyond this flow is confined by other boundary layers and is not independent of the flow at the walls. Because of this, boundary layers emerge around the perimeter, which ultimately results in the formation of a core zone. Investigations of internal flow are made more difficult because the two are connected in most situations. Many assumptions are made regarding the core region [Jaluria, 1980], which is done to make the problem easier to understand.

The size of the area determines the flow structure, character, and heat transfer rate during natural convection in a restricted space. This is because all of these factors are determined by the flow. For instance, the liquid temperature will vary in the tube cross-section and along the channel as it moves from one end to the other. In addition, at some distance from the opening of the tube, the fluid will be subjected to the influence of viscous forces, which will cause it to move more slowly. As the boundary layer approaches the walls of the enclosure, it becomes denser and eventually forms. The boundary layer covers the hydrodynamically stable tube

region, which also fills the cross-section. When the boundary layers of a fluid with constant liquid physical properties combine, a dimensionless typical velocity distribution of the given flow regime is produced. This distribution does not take into account any dimensions. It has been discovered that this particular distribution of velocity characterizes the flow regime. The quantity of heat transferred from the surface to the interior is increased using ribs, which leads to enhanced cooling. Calculating the amount of heat transported in systems such as these is achievable once the data are processed in such a way that they apply to smooth channels.

An approach based on the calculation of heat transfer in an analogous tube with a circular cross-section can be used to estimate the amount of heat transfer that occurs in tubes with a cross-section that is not a circle. Martynenko and Khramstova [2005] is the cited source.

It consists of a surface with a constant temperature (Tw) and an initial temperature (to) at the inlet of the flow. The temperature disparity creates a density difference between the fluid and the wall, leading to a buoyancy field within the tube. Regardless of the pressure difference between input and output, fluid in the tube will continue to flow freely due to the buoyancy force.

There is a dynamic relationship between buoyancy and speed in the water. For buoyancy to be effective, it is necessary to have other forces acting on the object, such as gravity (g) per unit mass.

The intake region of a circular tube is the primary focus of our inquiry because this is where laminar flow and heat transfer are most likely to occur. The governing continuity, momentum, and energy equations will be solved numerically by employing the finite difference method. An investigation will be conducted into the thermal boundary conditions of a constant wall temperature (CWT) and a constant heat flux (CHF). The Excel program will be used to compute everything pertaining to the flow of fluids and the transfer of heat.

1.1.2. Internal Forced Convection

Boundary layers form on the inner surface of a passage when forced convection is applied from within [8]. The passage of fluid through a tube between two plates is a common occurrence. Figure 1.1 shows the development of the hydrodynamic boundary layer (as a result of viscosity) for flow entering a circular tube (two flat plates placed side by side). The boundary layer of a tube (or plate) begins at its mouth and grows as the tube (or plate) is filled with fluid. There is a constant change to the velocity profile inside the initial opening of the tube (or plate). The flow is said to be “hydrodynamically fully developed” when the thickness of the boundary is equal to the radius of the tube (or half-spacing between the two plates). As the flow matures, its velocity profile becomes uniform. For a laminar flow, the Reynolds number is equal to approximately 5% of the ratio of the entrance length to the diameter of the tube (based on the tube diameter). Because of this, the entrance length grows along with the Reynolds number (because a thinner boundary layer requires a longer distance for the boundary layer to merge). Shear stress, as shown in Figure 1.1, rises with an increasing Reynolds number and decreases from the inlet of the tube to a constant value once the flow has reached its fully developed condition (because of a thinner boundary layer from the entrance and the long entrance length). Calculating the entrance length for a turbulent flow, which is typically between 10 and 20 times the diameter of the tube, is more challenging. The development of turbulent flow downstream of a tube diameter of 10-20 times is difficult to detect.

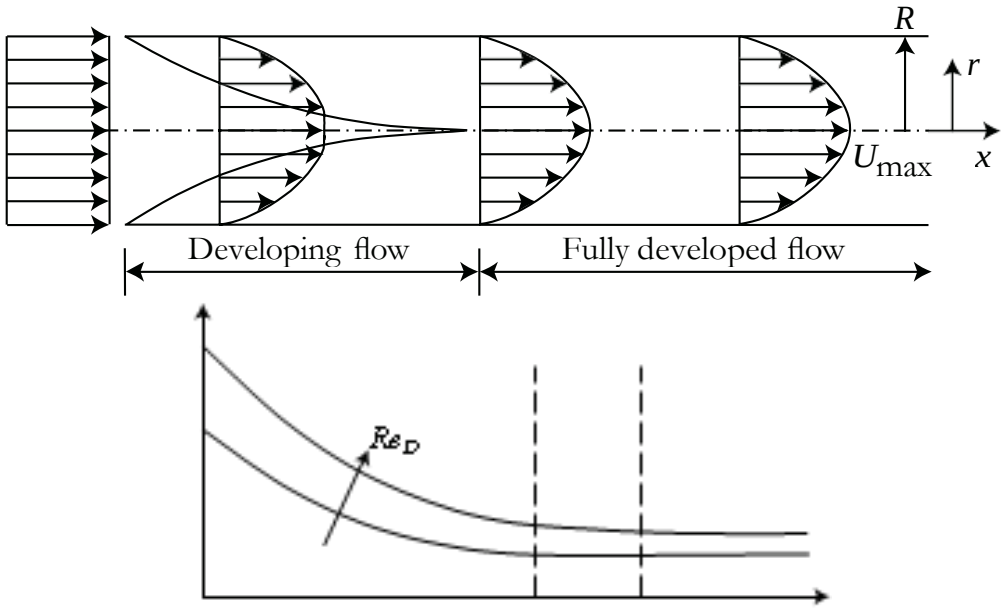

Figure 1.1. Shear force and speed in a circular cylinder between two surfaces [8].

The growth of the thermal boundary layer (because of thermal conductivity and velocity) for flow into a circular tube is shown in Figure 1.2 (between two parallel plates). Initially forming at the opening of the tube (or plate), the thermal boundary layer expands longitudinally. As more heat is added along the wall of the tube (or plate), the temperature profile shifts further away from the entry. When the thickness of the thermal boundary equals the radius of the tube, the flow is said to be thermally fully developed (or half-spacing between the two plates). After reaching thermal maturity, there is no further change to the dimensionless temperature profile (despite the increasing temperature).

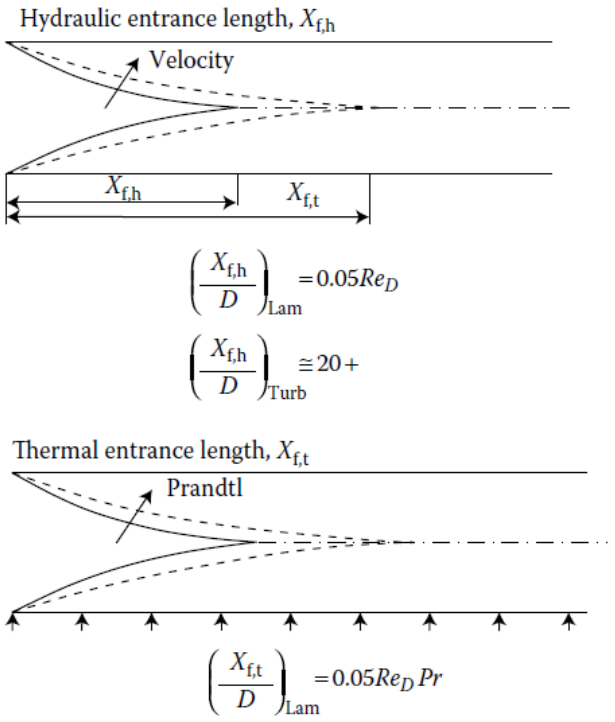

Figure 1.2. Hydraulic or thermal entrance lengths in circular tubes or between two surfaces [8].

1.1.3. External Natural Convection

This refers to a type of flow in which the motion of the fluid is determined not by an external force but by the relative densities of its constituent parts. This applies to liquids and gases (such as in a pump, fan, suction device, etc.), this typically leading to natural circulation, which is the ability of a fluid to circulate continuously in a system despite being affected by factors such as gravity and potential changes in heat energy. The force of gravity primarily triggers convection in nature. If, for example, a layer of hotter, less dense air sits atop a layer of colder, denser air, the more desirable, less dense air will rise and replace the colder, denser air as the top layer is pulled downward by gravity at a greater rate. This mixing leads to convection. Due to its reliance on gravity, convection cannot occur in weightless (inertial) environments such as the International Space Station in orbit. Natural convection occurs when there are hot and cold regions in either air or water, as water and air become less dense when heated. For example, since salt water is denser than fresh water, a layer of salt water superimposed on a layer of fresher water will also cause convection in the world's oceans (see Figure 1.3) [9].

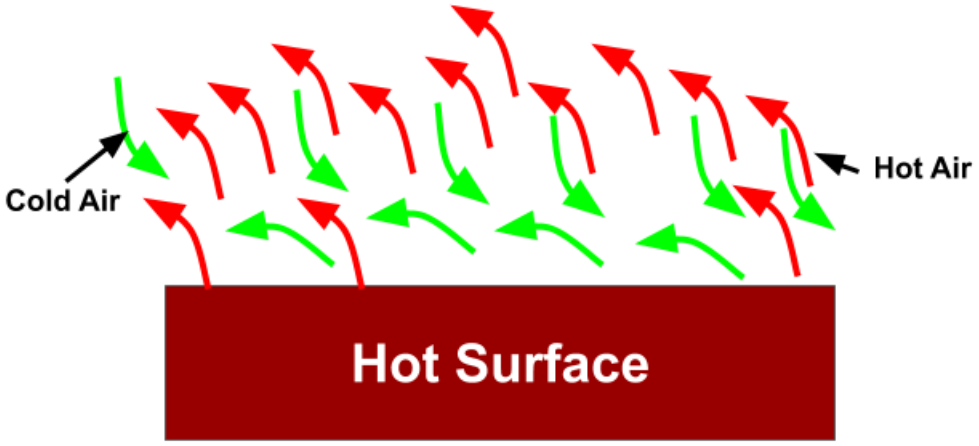

Figure 1.3. External natural convection [9].

Natural convection is a topic of intense study because of its occurrence in nature and its practical applications. In all natural weather systems, convection cells, which form when air rises above heated land or water, play a crucial role. Rising hot air plumes from fires, oceanic currents (the tourmaline circulation), and the creation of sea winds are all examples of convection (where Coriolis forces also modify upward convection). Many engineering processes rely on convection, such as the cooling of molten metals and the flow of fluids through covered heat-dissipation fins and solar ponds. Natural convection, which uses airflow rather than mechanical fans, is widely used in industry. This phenomenon applies to devices large and small, from computer chips to industrial cooling systems.

It is more likely that natural convection will occur and proceed quickly if there is a larger density difference between the two fluids, if the acceleration caused by gravity driving the convection is larger, or if there is a larger distance across the conducting medium. Neither the likelihood of nor the velocity of natural convection will improve with increased viscosity (stickiness) of the fluid or faster diffusion (which eliminates the heat gradient creating the convection). When natural convection starts, the Rayleigh number (Ra) can indicate this. When buoyancy differences within a fluid arise from factors other than temperature fluctuations, the resulting fluid motion is known as gravitational convection (see below). On the other hand, natural convection and other buoyant convection processes do not occur in microgravity

environments. These activities require conditions that generate gravitational acceleration (proper acceleration).

The varying densities of the fluid serve as the primary motive force. If the density changes are caused by heat, the driving force is called a “thermal head” or “thermal driving head.” In a fluid system designed for unintentional circulation, there will be both a heat source and a heat sink. They are all in contact with a portion of the system fluid but not the entire system. If it becomes necessary to remove excess heat, a heat sink may be placed in a higher location than the heat generator.

Materials that are fluid at room temperature tend to expand and lose density when heated. As a result, they decrease in temperature and become denser. Fluid that has been heated becomes lighter than the surrounding fluids and therefore rises at the heat source of a natural circulation system. Since gravity pulls objects downward, the fluid in the area cools and densifies at the heat sink. The combination of these phenomena results in fluid circulation between the heat source and the heat sink.

1.1.4. External Forced Convection

In forced convective heat transfer, an outside force, such as a fan or pump, causes fluid or air to move. The heat transmission rate is higher with forced convection than with natural convection [10].

Forced convection heat transfer rates are influenced by air velocity. The heat transmission rate will increase with increasing air velocity (Figure 1.4).

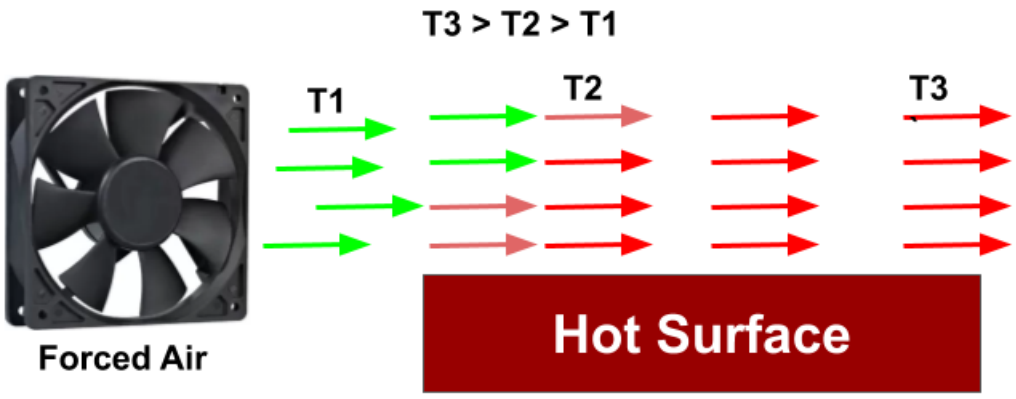

Figure 1.4. External forced convection [10].

Both conductive heat transfer and fluid motion are involved in forced convection. An air conditioner, for instance, uses forced convection to chill a space. The rate of room cooling will also increase as the AC fan speed increases due to a rise in the heat transfer coefficient.

Examples of forced convection applications include [11]:

1. Movement of coolant in an automobile engine;
2. Employing a fan to cool a computer or laptop processor;
3. Heat exchangers;
4. Conditioning systems;
5. Hairdryers;
6. Electrical device cooling, including that of servers; and
7. Vehicle radiators, etc.

Convection requires fluid motion to occur. Forced convection is the term used to describe a convective heat transfer method in which the necessary fluid motion is produced using an external agent (such as a blower or fan) (Figure 1.5).

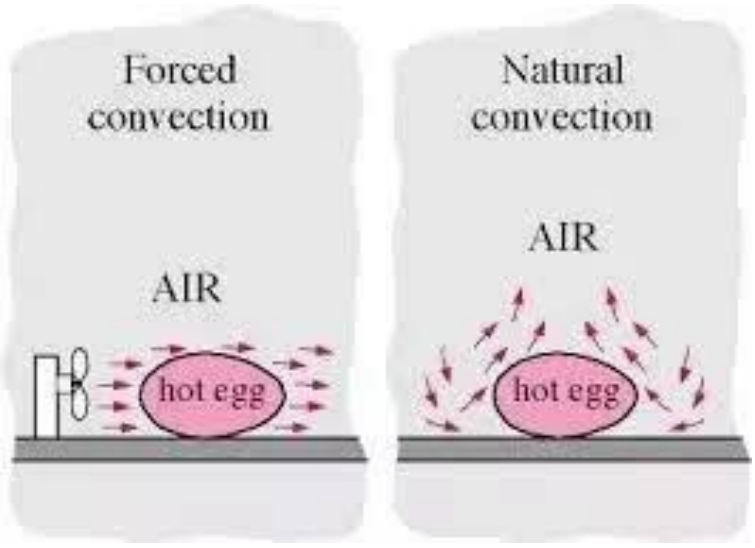

Figure 1.5. Difference between external forced convection and natural convection [11].

A higher heat transfer coefficient produces a lower heat transfer rate for a given heat source. To illustrate, some hot food on a plate can be cooled by blowing air over it. In contrast to natural convection, the heat transfer rate is increased in this case due to

the use of forced convection. The increased heat transfer rates in forced convection are due to the immediate removal of the hot air around the heated body by the air flow around it. Therefore, the heat transfer coefficient for induced convection is greater than for natural convection.

1.2. MATERIAL AND METHODS

1.2.1. The Tubular Heaters

An electrical heater heats a vertically thin cylinder. Three separate electrical tube heaters were used in all three experimental thin vertical cylinders. These heaters were then positioned to provide a homogeneous heat flow to the walls of the cylinders. Dimensionally, the three tube heaters were of identical size. The outer cylinders and the tubular heaters were similar in length, measuring 900 millimeters [13,14]. This length only serves as an active heated length of 900 millimeters. Copper was used in constructing the tubular heater due to its high thermal conductivity. The heater was composed of wire resistant to nickel and chromium in equal proportions, with the wire attached to terminal pins and centered in the metal tube. After filling the tube with high-quality magnesium oxide, it was crushed to transfer heat rapidly. A ceramic bush was employed to block the flow of electrical current and ensure that the terminal pins were correctly insulated. The three heaters were connected in parallel, as shown in Figure 4.3, to supply a total power of approximately 800 W.

1.2.2. Magnesium Oxide

Due to its better capabilities in electrical insulation, magnesium oxide was used in the tubular heater. As shown in Figure 1.6, magnesium oxide (MgO) was used to fill the tube immediately after the coil was inserted into the sheath to prevent the coil from coming into contact with the sheath. The tubular heater was vibrated while being filled to ensure that the MgO filled the vacant space between the sheath and the coil.

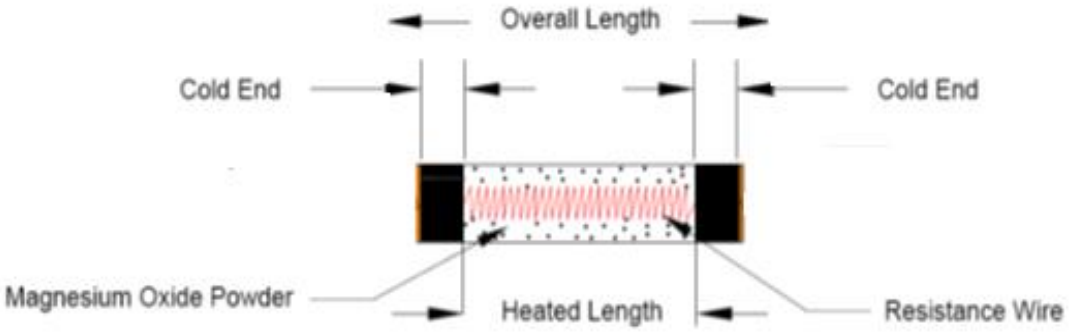

Figure 1.6. Tubular heater.

1.2.3. Variac

Variac is a single-coil variable autotransformer that uses the same coil for both the primary and secondary windings [15]. To perform the same functions as ordinary transformers but with lower voltages, variable autotransformers are utilized. Unlike normal autotransformers, they are also fitted with automated switchgear that automatically steps a voltage up or down depending on pre-set conditions. Automatic voltage regulation for industrial equipment, simulation of power line conditions, and control of switches reliant on external events can be achieved with the use of variable autotransformers. Variable autotransformers are an automatic replacement for standard autotransformers and may be used anywhere a regular transformer can be used. They are smaller, lighter, and less expensive than conventional capacitors and can handle voltages as low as 25 volts and as high as 200 volts. Voltage regulation for the thin vertical cylinders can be automatically utilized as a variac (as in Figure 4.2 (autotransformer)). The heaters are linked to the controller to manage the voltage and power.

1.2.4. Liquid Pump

A small pump was placed at the bottom of the tank to pump liquid to the cylinder from the bottom [16]. The pump operates on a constant DC current. Therefore, a DC-AC converter was used to prepare a constant direct current for the pump. The power supplied to the pump was calculated using a Wattmeter with an average power of 40 W being supplied to the pump, as shown in Figure 1.7.

(a) (b) (c)

Figure 1.7. (a) DC-AC converter, (b) Wattmeter and (c) liquid pump.

1.2.5. Gate Valve

A gate valve was placed between the pump and the water flow sensor to change the gate opening to obtain different flow rates and thus obtain different Reynolds numbers [17]. The gate valve is shown in Figure 4.2.

1.3. MEASUREMENTS

The following is a classification of results measurement that have been obtained throughout the course of the tests.

1.3.1. Temperature Measurement

The temperatures at various locations on the surface of the thin vertical cylinders were measured using K-type thermocouples connected to a 10-channel temperature recorder, as shown in Figure 4.2. The mean temperatures of the fluid (water) were also measured at the inlet and outlet of the large cylinder.

1.3.2. Flow Rate Measurement

A water flow sensor was used to measure the flow of water. It was placed in the stream of water coming from the pump and going to the entrance hole at the bottom of the cylinder. The sensor was very close to the hole to measure the flow rate of the liquid. At the same time, it would enter the cylinder. It was also wrapped with a silver label sticker that insulated the liquids and heat, merely as a precaution (see Figure 4.2).

1.3.3. Input Voltage and Current

Heater wires were connected to the variac with one wire being associated with a digital clamp-on multimeter to measure the input current. In contrast, the voltage was measured by determining it with the variac, and the variac device also contained a digital screen indicating the voltage. Figure 4.2 shows the instrumentation.

1.4. OBJECTIVES

The following objectives have been achieved through this thesis:

1. A study of the effect of the flow rate of water on the heat transfer rate from a cylinder placed in the middle of several cylinders on its sides identical to it.

2. An investigation of the effect of the flow rate of water on the heat transfer rate from the side cylinders.

3. An extraction of the characterization of the average Nusselt numbers through the experimental correlations of the middle and side cylinders.

4. Making a comparison between the final results for both middle and side cylinders and making a comparison for cylinder surface temperatures between the current study and a previous study that was made on natural convection.

5. Using forced convection to accomplish the heating and reaching the average Reynolds number range to a value greater than 200.

1.5. THESIS STRUCTURE

This study consists of five main parts. An introduction and general information about heat transfer by convection are presented in Part 1. Literature related to this study is presented in Part 2. The theoretical base relations of external forced convection heat transfer in tube banks are presented in Part 3. The experiment and its method are explained in Part 4. The Results and discussion are presented in Part 5. Finally, conclusions are given in Part 6.

PART 2

LITERATURE REVIEW

A review of previous research looked at the impact of fluids on convective heat transfer inside a tube bank filled with fluid, both theoretically and experimentally. Circular tubes are almost always utilized as the foundation of heat exchangers because of their simplicity and low production cost. Since streamlined circular tubes may separate and create significant wakes which can result in high-pressure drops, they have a much lower hydraulic respect and understanding and thus need less pumping power.

2.1. FORCED CONVECTION HEAT

Local heat transfer coefficients for forced convection in Seban and Drake elliptic tubes at small inclination angles (0-6 degrees) were reported [18,19].

The effects of Re = 40 and Re = 80 on the results of unsteady forced and natural convection heat transfer from horizontal circular and elliptic tubes were studied by Kikkawa and Ohnishi [20]. The two-dimensional Navier-Stokes and energy equations were numerically solved after a detailed experimental thermal field analysis.

Ota et al. [21,22] evaluated the airflow behavior and heat transfer characteristics for two different elliptic tube axis ratios, namely 1:2 and 1:3. Angles of attack between 0 and 90 degrees were considered in this study, with the Reynolds numbers varying from 8,000 to 79,000. It was found that a separation angle of 60 to 90 degrees was optimal to maximize the average heat transfer coefficient. This proved to be the case when they analyzed their data. It was found that the minimum means of the heat transfer rate of the elliptical tube were higher than those of the circular tube.

Nishiyama et al. [23] found that when two elliptical tubes with an axis ratio of 1:2 are placed next to one another and subjected to cross-flow, the local heat transfer coefficient was significantly affected by the angle of attack and tube spacing.

The shell side of an oval tube bank would reduce pressure and improve heat transfer, as reported by Merker and Hanke [24]. They found that the frontal areas of shell-side heat exchangers were significantly smaller for oval-tubed designs than for circular-tubed designs.

Ilgarubis et al. [25] presented the operation of elliptical finned tubes using forced convection. Various Reynolds numbers, from 4 to 103, were tested experimentally to learn more about the unique qualities of the heat transfer at each level.

Prasad et al. [26] found that pressure and heat transfer were reduced when the flow was perpendicular to the airfoil. Compared to a round tube, the Stanton numbers to pressure failure criterion were higher when the NACA-0024 was used as the airfoil test section. A sphere tube was used as a standard for comparison.

Badr and Shamsher calculated free convection from isothermal horizontal elliptic tubes. In both cases, full conservation equations of mass, momentum, and energy had to be solved before any boundary-layer simplifications could be made. Badr and Shamsher solved free convection from an ellipsoidal tube for Rayleigh numbers between 10 and 103 and axis ratios between 0.1 and 0.964 [27,28].

Rocha et al. [29] compared one-row tubes with plate-fin heat exchangers that were either elliptical or circular. A notable improvement in efficiency was observed with elliptic tubes. Compared to circular tubes, heat transfer increased by 18% when using elliptical tubes.

Badr described forced convection heat transfer in an isentropic, cross-flowing elliptical tube. The range of Reynolds numbers and angles of attack studied in this article was from 0° to 90° and 2,000. Between 0.4 and 0.9 tube axis ratios were possible. According to the results, heat transfer was quickest at 0° and slowest at 90° [30].

Pressure drop tests on single, double, and triple-row elliptical, circular, and plate-fin heat exchangers were conducted by Bordalo and Saboya [31]. The latter test had a lower pressure drop when comparing elliptical and circular tubes. The pressure drop coefficient in the tubes could be decreased by 30% with the elliptical arrangement.

The flow over an in-line array of elliptic tubes that were cross-flown at a ratio of 1:2 was studied by Castiglia et al. [32]. Compared to a similar circular tube arrangement, this configuration would create significantly less turbulent air.

Badr et al. calculated the form drag and skin friction in different orientations with the major axis in the flow direction for an oval tube [33]. When Re = 700, the total drag coefficient for an oval with a minor axis length ratio of 0.6 is 0.9, but it drops to 0.8 when Re = 3,700. The primary reason for an object's resistance is its shape. Drag can be reduced with thinner oval tubes or other shape factors. It has been found that rectangular tubes have 10-20% less resistance than their circular counterparts.

Hasan and Siren [34] experimented to determine whether plain circular tubes or oval tubes performed better in evaporative cooling heat exchangers and it was found that oval tubes were more efficient. For oval tubes, the average Colburn factor for mass transfer was between 1.93 and 1.96, while for circular tubes, it was between 0.50 and 1. Oval tubes would perform better in terms of thermal and hydraulic efficiency than their round counterparts.

Based on what has been shared by Tiwari et al. [35], to calculate the flow structure and heat transfer in a tubular heat exchanger with an integrated oval tube and delta wing vortex generators, a three-dimensional computational study of forced convection heat transfer was conducted. Forced heat convection was used in this study. The researchers discovered that fin tube heat exchangers could benefit from adding oval tubes and vortex generators.

Heat transfer for a staggered arrangement of circular and elliptic finned tubes in external flow was studied by Matos et al. [36] using numerical and experimental methods. The most efficient method of heat transfer was found to be through elliptical tubes. Compared to the best circular tube arrangement, heat transfer was 19% better when the tubes were arranged in the best elliptical configuration. The

elliptical configuration could potentially improve global performance at a lower cost due to enhanced heat transfer and a 32% reduction in mass. Mass can be decreased by 32% due to the use of elliptical configurations.

Experiments and numerical simulations were used by Bouris et al. [37] to explore the novel tube bank heat exchanger's thermal, hydraulic, and fouling characteristics. The morphology of deposits could be used to create a tube that effectively reduces fouling. Their innovation reduced deposits by 75% and the pressure dropped by 40%, all while improving heat transfer by an order of magnitude.

2.2. MIXED TUBE

Empirical research on the flow and thermal performance of a tube encased in two cross-flow tubes was conducted by Aiba and Yamazaki [38]. Each note had a pitch ratio of 1.3% to 5%. In the temperature range of 1.3°K to 3.8°K, the vortex region of the first tube had a greater impact on heat transfer.

Four-cylinder flow was analyzed by Aiba et al. [39] over $104 < Re < 5{,}104$ with pitch ratios ranging from 1.15 to 3.4. The Nusselt number changed over a significant Reynolds number range.

Heat transfer was investigated by Aiba et al. [21] for $104 < Re < 6{,}104$ tube banks with seven-tube spacings. A constant mean Nusselt number was recorded in the downstream tubes (including the second tube).

Zukauskas and Ulinskas [40] analyzed the differences in pressure drop and heat transfer between tube banks with different pitch ratios. There was some advice to change the form of the heat exchanger.

Flow characteristics in straight, triangular, square, and offset circular tubes were investigated by Zdrakovich [41]. Staggered wing, ellipsoidal, and cylindrical shapes were tested for thermal efficiency and drag coefficient by Horvat et al. [42].

This tube was developed by Nouri-Borujerdi and Lavasani [43]. At various angles of attack, the thermal performance and flow around the cam-shaped tube were

analyzed (r). In every range except for 90 and 120, the tube performed better than a circular tube.

Turbulent flow through a set of five elliptical tubes was investigated experimentally and numerically by Ibrahim and Gomma [44]. 5,600 Re 40 employed four minor-to-major axis ratios, each optimized for a specific angle of attack. Up to an angle of 90° of attack, the convective heat transfer coefficient would grow. The temperature range in which thermal performance was optimal was 0 to 90. These were the results of yet another carefully orchestrated scientific study.

Heat transfer in cross-flowing triangular cylinders was studied by Ali et al. [45], who found that high Reynolds numbers would transfer heat more quickly through triangular tubes than through circular tubes.

The flow and heat transfer in a small circular and oval finned-tube heat exchanger were numerically analyzed by Han et al. [46]. The fins were louvered and wavy, and heat transfer was found to be 4.9% better with the oval-tube fin than with the circle-tube louver fin.

Using numerical methods, Swain and Das [47] investigated the flow over elliptical and flattened tube banks with pitch-to-diameter ratios between 200 and 2,000. In both in-line and staggered configurations, the pressure loss and heat transfer coefficient were found to be minimized by increasing the pitch.

Using wing-shaped tubes as a heat exchange medium was a topic of study for Sayed Ahmed et al. [48]. Maximum effectiveness was reached at the value of 0. When compared to circular tubes of the same cross-sectional area, the average Nusselt number was 24% higher.

Cam-shaped tube flow over a stepped bank was investigated by Bayat et al. [49]. Higher Nusselt numbers and smaller pressure drops were found in cam-shaped tubes compared to their circular counterparts. Cam-shaped tube bundles in in-line arrays were found to perform better than circular banks, as discovered by Lavasani et al. [50].

The thermal efficiency of two cam-shaped tubes in a side-by-side arrangement with different pitch ratios was determined by Lavasani and Bayat [35]. The pitch ratio was found to have improved heat transfer. Tandem cam-shaped tubes were studied numerically [36] to determine the pitch ratios and drag coefficients.

Sun and Zhang [51] conducted a numerical investigation into the impact of the axis ratio on the efficiency of elliptical finned tube heat exchangers. It was found that increasing the axis ratio would boost thermal-hydraulic efficiency to achieve a constant air velocity.

Zhang et al. [52] studied thermal performance and flow over an egg-shaped tube with varying aspect ratios (4,000 Re 50,000). At high Re values (> 11,952), the best thermal performance was seen in tubes with an axis ratio of 2.

The Nusselt number and drag coefficient of a single-row, cylindrical, variable-pitch wing were numerically determined by Sahim [53]. The transverse distance was found to have reduced the drag. The least amount of room between each cylinder was observed to have maximized efficiency.

Kong et al. [54] computed flow over tube bundles with slotted and flat fins. Regardless of the slot-to-fin-pitch ratio, tubes with slotted fins were observed to be the most thermally efficient design.

The effect of blockage ratios on flow in a cam-shaped tube was studied by Lavasani et al. [55] at Reynolds numbers ranging from 7,500 to 17,500. The study showed that drag experienced by a cam-shaped tube diminished as the blockage ratio increased. Both thermally and hydraulically, cam-shaped tubes would outperform circular tubes across a wide range of blockage ratios.

Deepakkumar and Jayavel [56] tested a heat exchanger with circular and elliptical finned tubes. This three-dimensional numerical simulation analyzed the impact of inlet velocities on thermal performance and flow characteristics.

Gholami et al. [57] utilized fin and oval tubes as part of their numerical tube bundle. The new layout enhanced heat transfer and reduced pressure drops. It was found that fins could increase the Nusselt number by 20%.

Mangrulkar et al. [58] conducted a numerical and experimental study and found that for Re = 5,500, the Nusselt number could be improved by 50% by adding a splitter plate to a bank of circular cylinders. The ratio of the splitter plate length to the tube diameter (L/D) was 1, and the Reynolds number ranged from 5,500 to 14,500.

A numerical study was conducted by Mangrulkar et al. [59] to enhance the friction factor and thermal performance of cam-shaped tubes for the operating temperature range of 11,500 to 42,000. Heat was found to transfer more rapidly in cam-shaped cylinders than in conventional circular cylinders. Reduced friction was especially noticeable in comparison to the circular cylinders.

The thermal efficiency of mixed-tube banks was studied by Mohanty et al. [60] at 100-2,000 Re and 1.25-1.85 pitch ratios. It was found that pressure loss and heat transfer were both greater in the staggered arrangement than in the in-line configuration.

Heat exchangers with flat tubes and fins of varying shapes (such as wavy, plain and rectangular) were tested by Moorthy et al. [47]. The heat exchangers stood in a line and at staggered intervals. The friction factor and the Nusselt number were both greater for the fins that were not aligned. The results were poorest for the rectangular fin.

Khalifa and Hussien [61] proved that naturally occurring convective heat transfer occurs in water-immersed heat exchangers. Three cylinders would comprise each row in a square with a 2:1 pitch-to-diameter ratio. It was found that there is an empirical connection between the Nusselt and average individualized Rayleigh numbers. The surface of the cylinder would cool as a result. The researchers compared the surface temperatures for the middle cylinder (in the highest flow rate for this current study) to other available data.

PART 3

THEORETICAL BASE OF THE STUDY

3.1. HEAT TRANSFER MODES

Total heat transfer [62,64,63] from a thin vertical cylinder can be calculated as:

$$Q = Q_{cond} + \mathbf{Q}_{conv} + Q_{rad} \tag{3.1}$$

3.1.1. Conduction Heat Transfer

Calculating the amount of heat transferred by conduction can actually be carried out using Fourier's Law [62,64,63]:

$$Q_{cond} = -k\,A\frac{\partial T}{\partial x} \tag{3.2}$$

where k is thermal conductivity, the heat transfer area is A, and the temperature gradient or slope of the temperature profile is $\partial T/\partial x$. As will be seen in the following section, the conduction of heat can occur in this scenario at one of three different points:

1. Transfer of heat from an external heat source to the surfaces of stainless steel cylinders: It is difficult to measure the surface temperature of the tubular heater while it is contained within a stainless steel cylinder and also because the distance between the tubular heater and the cylinder is minimal and filled with MgO (k = 30 W(m.°C)). The conduction losses that occur between the tubular heater and the stainless steel cylinder are disregarded.
2. The bottom ceramic pipe does not receive any heat from the tubular heater since there is no temperature difference between the end of the heater and the cylinders.
3. The top ceramic pipe does not receive heated since there is no temperature difference between the end of the tubular heater and the cylinders.

3.1.2. Radiation Heat Transfer

Calculations for heat transmission by radiation from the surface of a stainless steel cylinder are as follows [62,64,63]:

$$Q_{rad} = \varepsilon\, A\, \sigma\, F\ \ (T_{sav}^4 - T_m^4) \tag{3.3}$$

where ε is the emissivity of the worn stainless steel, σ is the Stefan-Boltzmann constant (5.66×10^{-8} W/m^2 K4), F is the form factor, T_{sav} is the average surface temperature of the cylinder, and T_{m} is the mean temperature of the water in Kelvin. Radiation-related heat transfer was calculated at typical temperatures and determined to account for less than 3% of all heat transfer (sample of error is presented in Appendix C); hence it was disregarded.

3.1.3. Convection Heat Transfer

It was shown that convection transfers nearly 97% of the total heat to the fluid, as seen in Appendix C. Equation 3.1 can be condensed into the following by ignoring the losses in heat transmission caused by conduction and radiation heat transfer [62,64]:

$$Q = \mathbf{Q}_{conv} = h\, A_{\mathrm{S}}\, \Delta T_{\mathrm{in}} \tag{3.4}$$

3.2. GOVERNING EQUATIONS

Since we used a set of cylinders with small diameters placed inside a cylinder container with an inlet hole and an exit hole, we can say that the device is a shell and tubes, so we use the equations of the tube bank. All equations that were used are explained in more detail in Part 3 and their sources will also be clarified [12].

3.3. CALCULATION PROCEDURE

According to Holman [63] and Cengel [62,64] et al., the physical characteristics of water are computed using mean temperature and average surface temperatures, as in Eq. 3.5 and Eq. 3.6:

$$T_{\mathrm{m}} = \frac{T_i + T_e}{2} \tag{3.5}$$

$$T_{sav} = \frac{T_{s1} + T_{s2} + T_{s3}}{3} \tag{3.6}$$

From T_{m} and from the table (in Appendix A), we get (μ, Pr), and from T_{sav} and the same table, we get Pr_S, while the value of the density of water (ρ) was constant (998.23 kg/m^3) at an atmospheric pressure of 1 atm [62,64].

Most of the values of T_{m} and T_{sav} were not identical to those in the table, so the average value for them was taken from Eq. 3.7. Taking the viscosity (μ) as an example:

$$\frac{T_2 - T_{\mathrm{m}}}{T_2 - T_1} = \frac{\mu_2 - \mu_x}{\mu_2 - \mu_1} \tag{3.7}$$

where μ_x was the extracted value used in solving mathematics problems and making curves.

The Average Reynold number was calculated using Eq. 3.8 as follows [62,64]:

$$Re_D = \frac{\rho\, V_{max} D}{\mu} \tag{3.8}$$

$$V_{max} = \frac{S_T}{S_T - D} V \tag{3.9}$$

$$V = \frac{\dot{V}}{(N_T\, S_T\, L)} \tag{3.10}$$

To convert the flow rate that we measured to the volume flow rate, we convert the units from L⁄M to m^3/s using Eq. 3.11:

$$\dot{V} = Q \times \frac{10^{-3}}{60} \tag{3.11}$$

The following steps were taken to arrive at the average Nusselt Number using Eq. 3.13 [62,64]:

$$Nu_D = \frac{h\, D}{K_f} = C\, {Re_D}^{m}\, Pr^n\, (\, Pr\, /\, Pr_s\,)^{\,0.25} \tag{3.12}$$

$$Nu_{D,\,NL} = \mathrm{F}\, Nu_D \tag{3.13}$$

C, *m*, *n*, and F are determined from the tables in Appendix B and the heat flux was determined using Eq. 3.14 [62, 64,63]:

$$q'' = \frac{P}{A_S} \tag{3.14}$$

$$P = I * V \tag{3.15}$$

$$A_S = N\pi DL \tag{3.16}$$

The pumping power required can be determined with Eq. 3.17 and the pressure drop with Eq. 3.18 [62, 64]:

$$\dot{W}_P = \dot{V}\Delta P \tag{3.17}$$

$$\Delta P = N_L f \chi \frac{\rho V^2_{max}}{2} \tag{3.18}$$

where (f,χ) was determined from the tables in Appendix B.

PART 4

METHODOLOGY

4.1. EXPERIMENTAL SETUP AND MEASUREMENT PROCEDURE

The experimental setup aims to investigate forced convection heat transfer from three hot, thin vertical cylinders submerged in water at various heat fluxes. In addition, the average Reynolds and Nusselt numbers for the average flow rates for these kinds of designs will be compared using experimental data. The methods that were followed to create the testing rig are explained in this section. The test rig was built with stainless steel heated cylinders, aluminum heated cylinders, tie rods, rubber pipes, electric wires, a liquid pump, a gate valve, a water flow sensor, a cylindrical stainless-steel container, thermocouples, a digital temperature recorder, a digital flow rate recorder, a digital clamp-on multimeter, thermal silicon sealant and a galvanized steel tank.

4.1.1. Experimental Procedure

Vertically submerging the assembly cylinders in the direction of gravity required the employment of a stationary water tank that was 42 centimeters in length, 42 centimeters in width, and 120 centimeters in height. After forcing water through the inlet hole at the bottom by the pump (with a rubber pipe), cold water would flow into a stainless steel cylinder which has a tube bank. This consists of nine thin vertical cylinders, three of which contained heaters and temperature sensors made from stainless steel, and six that were empty and made from aluminum before exiting through the exit holes in the top. The pump pushes the water that enters the inlet hole. One of the wires of the heater was linked to a digital clamp-on multimeter by a variac (Figure 4.2), allowing the user to control the input voltage flowing into the device. Thermocouple wires were linked to a digital temperature recorder so that temperatures could be read by the thermocouples (Figure 4.2). During the experiment, we were able to test the heaters at a variety of power levels by

monitoring the voltage that was being produced across the heaters by using the variable AC source. We used three different routes to produce a wide range of Reynolds numbers. The amount at which the gate valve was opening was changed three times, resulting in three distinct flow rate values (32.5 L/M, 25 L/M and 15.6 L/M); a small water flow sensor was used to demonstrate the flow rate to us. The input power of the heater was calculated by using the equation P = IV for the data collected from measurements of the voltage across the heater and the input current. Thermocouple and input power values were measured to analyze the steady-state heat transfer caused by forced convection within a boundary condition characterized by a constant heat flow. The Reynolds number was an additional dimensionless group that was explored with fluctuations in the Nusselt number to characterize forced convection, a characteristic of the phenomenon. This investigation was performed to learn more about forced convection.

The experimental rig was constructed from available materials. Figures 4.2 and 4.3 show the side view of the schematic diagram and the actual image of the experimental setup and the parts used.

4.1.2. Design and Fabrication of Three Thin Vertical Heated Cylinders

The stainless steel tube had an average thickness of 1.224 millimeters. Using stainless steel tubes with a high chromium content achieved good thermal conductivity and corrosion resistance. The cylinder was 900 millimeters long and 20 millimeters in diameter on the outside. Each cylinder had three evenly spaced holes bored into its interior. From the bottom up, the distances between the holes were 200 mm, 450 mm and 700 mm. Thin Type K fiber glass-insulated, thermocouple wires were inserted into the inner side of the cylinder wall. After that, the wires were readjusted so that their ends remained flush with the exterior of the cylinder. A tubular heater of identical length to the stainless steel cylinder was inserted inside it to provide heat, as shown in Figures 1.6 and 4.3. Magnesium oxide (MgO) insulated the area between the cylinder and the tubular heater. To prevent water from leaking into the cylinder, we used thermal silicon sealant to plug the holes in the cylinder. The 19 mm rubber pipe was used to house the electrical and thermocouple wires.

4.1.3. Configuration of Stainless-Steel Cylinders Assembly

A three-by-three array with a distance between the centers of two cylinders and a diameter ratio S_T/D of 2 was created (Figures 4.1 and 4.3) by employing two circular tube sheets, one on the top and one on the bottom, with holes for tie rods and the cylinders. The same cylinder configuration was preserved. The placement of eight tie rods at the tube sheet corners is shown in Figure 4.2. The assembly was housed inside of a stainless steel cylindrical container. The tie rods were solid steel rods used to maintain the spacing between the top and bottom tube sheets at the same level. This container had an outside diameter of 20 centimeters, a 2 cm diameter inlet hole at the bottom, and four 1 cm diameter exit holes at the top, as shown in Figure 4.2. The vertically aligned cylindrical assemblies were submerged in water and aligned with gravity. Galvanized steel was used to build the water tank, as seen in Figure 4.2, while Figure 4.1 shows how the cylinders were positioned around the central cylinder presenting the cylinder nomenclature. The surface temperatures of the three cylinders of the assembly (middle and side cylinders) were selected for measurement. Each of the three cylinders received a heating element as part of the installation. In addition, thermocouples were fastened so that the inlet and outlet temperatures of the water could be measured at the length of the container cylinder.

1. Side cylinders
2. Middle cylinder

Figure 4.1. Locations of the three heated cylinders in the assembly.

1. Thermo rubber tubing.
2. K-type thermocouples.
3. Heater wires.
4. Digital flow rate recorder.
5. Datalogger.
6. Variac.
7. Digital clamp meter.
8. Gate valve.
9. Liquid pump.
10. Pump wire.
11. Galvanized steel tank.
12. Top tube sheet.
13. Assembly cylinders.
14. Outlet holes.
15. Stainless steel cylinder.
16. Tie rods.
17. Inlet hole.
18. Bottom tube sheet.
19. Water flow sensor.
20. Tubular heater from the top.
21. Thermocouple tips.
22. Tubular heater from the bottom.
23. Stainless steel tubular heater.

Figure 4.2. Experimental setup visualization.

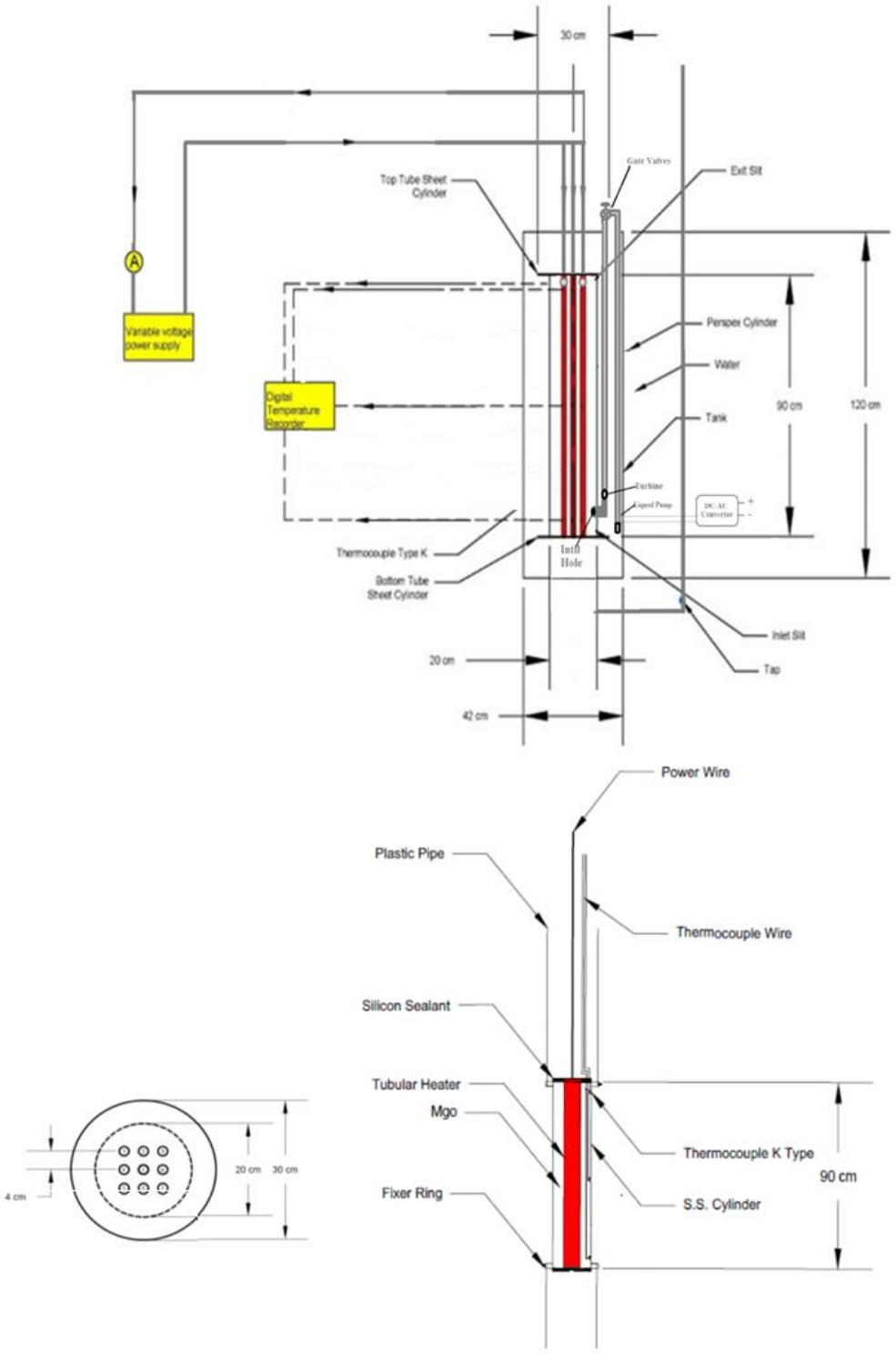

Figure 4.3. Side and top block diagram view and schematic diagram of the experimental setup for the cylinder and side view for the tubular heater.

The models and properties of the equipment of the experimental setup and the measurement instruments are seen in Table 4.1.

Table 4.1. Technical specifications of setup equipment and measurement instruments.

Devices	**Model and Properties**
Pump	Gross Fluid Transfer Pump 12-volt DC, 40 W
Wattmeter	Energy Consumption Meter Measuring Socket 230 V-3,680 W-16 A
Datalogger	Elimko Model E-680 Datalogger, Working ranges 20℃ to 75℃ - 25 V-200 V AC, standard working limits −200 + 1,300℃
Water flow sensor	1-60 L/min DC 5-24 V Hall Effect Water Flow Sensor
Stainless steel	16 BWG SS 304L
Thermocouple	Type K (copper constantan) with tips, fiberglass insulation −75℃--260℃**,** length 1.6 m
Variac	Input 220 V, output 0-250 V, 50 Hz, max. 4.5 A
Clamp meter	Dt-266 Pens Ampermetre (clamp Ampermetre - Multimetre - Avometre)

PART 5

RESULTS AND DISCUSSION

A cylinder assembly attached to a variable voltage regulator can be vertically installed in a tank (as illustrated in Figures 4.2 and 4.3). The variac supplied the cylinder heater with variable power ranging from 3.5 W to 840 W while maintaining the voltage. After fifteen minutes, it was noted that the surface temperatures were moving progressively closer to a condition of steady state, as indicated by the digital temperature. The tests were performed on nine uniform heat fluxes of 14.75 W/m^2, 206.417 W/m^2, 663.482 W/m^2, 1,179.52347 W/m^2, 1,990.44586 W/m^2, 2,830.85633 W/m^2, 3,818.71 W/m^2 and 4,953.99858 W/m^2. The first value was disregarded in the calculations because it was too small. A pump was installed on the exterior of the cylinder container to gather all the cylinders. This pump pulls liquid from the bottom of the tank and injects it into the cylinder from the bottom. In addition, a miniature water flow sensor was constructed on the exterior of the main cylinder that houses all the cylinders. It is essential to extract the Reynolds numbers just before the liquid enters the cylinder that measures the flow rate of the liquid. A gate valve was inserted between the water flow sensor and the pump, and measured three different flows by adjusting the amount of opening that the gate valve allowed to widen the scope of this study. When it was opened for the first time, the valve was fully open. When it was opened for the second and third times, it was partially open. The following effect was brought about by the three different flow rates: 32.5 L/M, 25 L/M, 15.6 L/M. The surface temperature changes along the vertical cylinders are shown in Figures 5.1 and 5.5. They can be seen at various axial distances from the bottom side and for various flow rates.

5.1. MIDDLE VERTICAL THIN CYLINDER IN WATER IN ASSEMBLY INDUCED CONVECTIVE HEAT TRANSFER

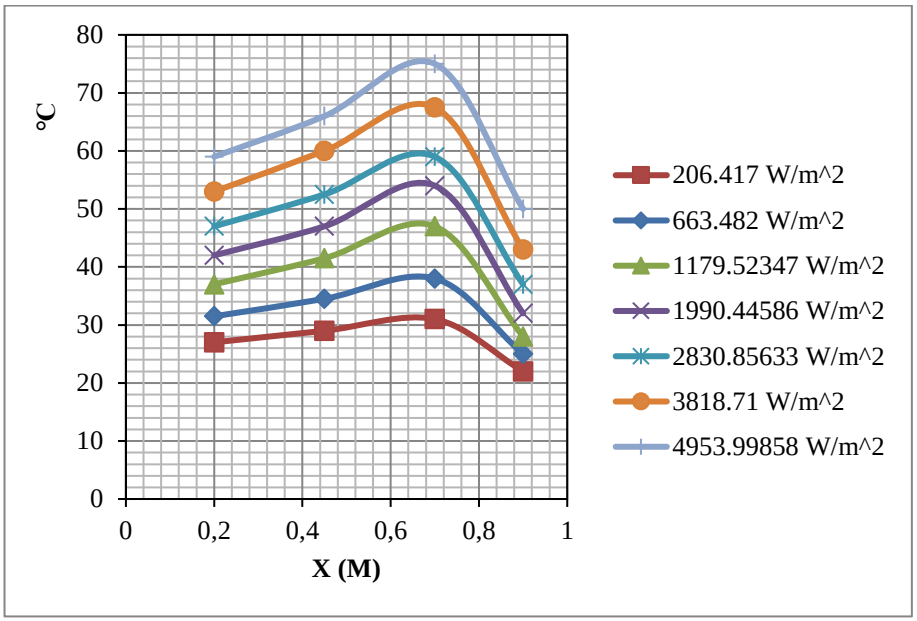

(a)

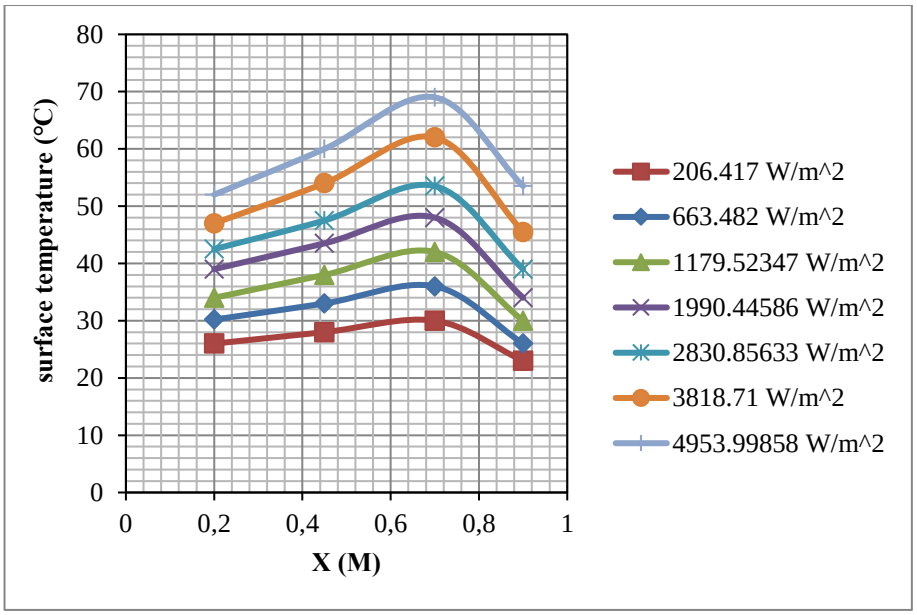

(b)

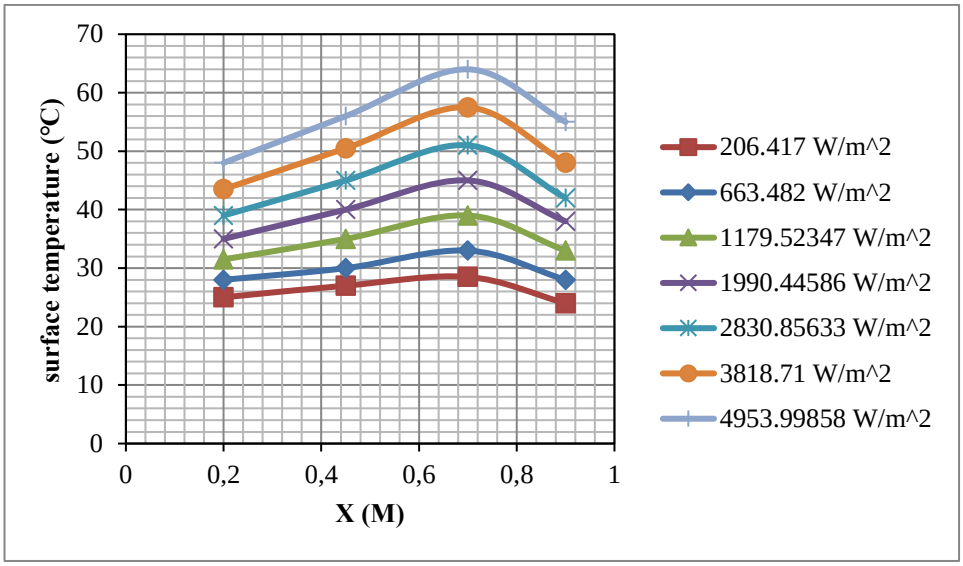

(c)

Figure 5.1. At varying uniform heat flux levels, surface temperatures at three axial points and in the outlet in the middle cylinder in the assembly were measured for flow rates of (a) 32.5 L/M, (b) 25 L/M, and (c) 15.6 L/M.

The delivery of a constant heat flux led to an increase in temperature along the cylinder axis, with higher surface temperatures at higher fluid flow rates and lower flow rates leading to higher water temperatures at the outlet (0.9 m). Therefore, heat transfer from the surface of the cylinder will take longer if the water flow rate is low. The following explains the overall shape and pattern of the distribution: while the surface temperature does increase with increasing axial distance, the temperature has reached its maximum at a distance of x = 700 mm. Surface temperature varies along the length of the cylinder for various reasons, the most important of which is the formation of a thermal boundary layer which can be thought of as a thermal insulator. There are three distinct causes for these temperature shifts. Because laminarization forms along the near wall of the cylinder, the boundary layer thicknesses start as clearly zero at the beginning of the heated length. This is due to the action moving along the near wall of the cylinder. This resultant situation naturally arises from the cylinder's cylindrical shape. It has been proposed that the surface temperature be raised in small, consistent increments, and it follows logically that the regional heat transfer coefficient will fall if the local surface temperature continues to increase. When the heat is dispersed uniformly throughout the cylinder,

the water temperature cannot rise any higher than it is now. Modifications to the physicochemical properties of the water are proportional to the temperature of the water. The immediate result is that the temperature can never again increase beyond its current high level. Since less friction is encountered during motion in water with a higher thermal conductivity, and radial flow increases, and there will be more friction to the flow of water if its thermal conductivity is lower than that of a viscous fluid. The viscosity of a liquid can serve as an indicator of its thermal conductivity. The boundary layer of hot water connects radially with cold water, and this is because of the rising of the hot water with the heated cylinder. As the water rises, the volume of the boundary layer increases because the water temperature increases with the altitude, and the local heat transfer rate decreases as a result.

For this reason, the cylinder's surface temperature will decrease, compared with those given by Khalifa and Hussien [61], and the results show that the two sets of data of the middle cylinder are in good agreement. The water around the middle cylinder has the highest flow compared to the water on the sides. Forced convection and natural convection differ in several ways, the most notable of which is the rate at which heat is transferred, as shown in Figure 5.2.

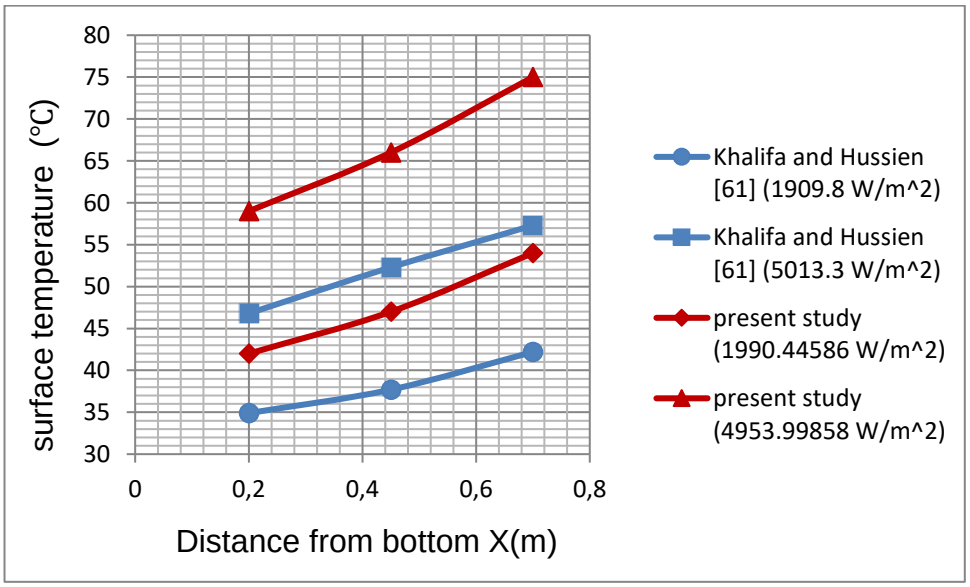

Figure 5.2. Comparison of surface temperatures at some roughly similar uniform heat flux values of previous natural convection studies for the middle cylinder in the assembly.

5.1.1. Correlations

The mean temperature and the average surface temperature were used as a starting point to determine the characteristics of the physical water and the surface of the cylinder. Nusselt and Reynolds numbers were utilized to determine whether or not there is a relationship between the forced convection heat transfer technology and dimensionless local numbers. The findings of this investigation are presented in this section when calculating the average Nusselt and Reynolds numbers that were determined for each flow rate. It was concluded that there is a relationship between the dimensionless numbers, which show the relationship between the average Nusselt number and the average Reynolds numbers. When exposed to various heat flows, the Nusselt number gradually increases with the Reynolds numbers. This was determined for each flow rate over $100.31 \leq Re_D \leq 278.14$. The accompanying image visually represents these results (Figure 5.3).

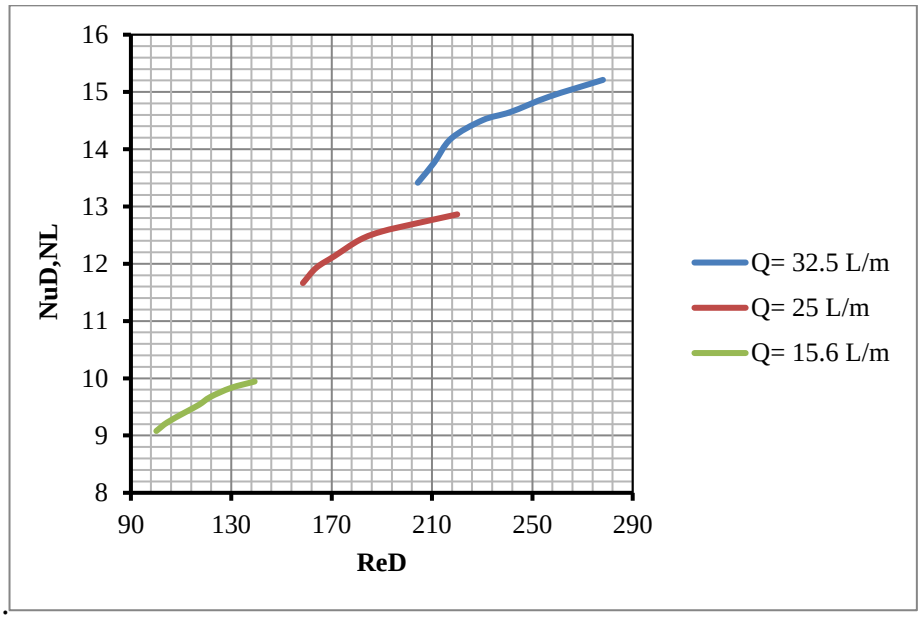

Figure 5.3. Average Nusselt and average Reynolds numbers at different heat fluxes at different flow rates for the middle cylinder in an assembly.

We also observe that the average Nusselt number rises as the flow rate rises, suggesting a direct correlation between the two quantities. Additionally, since the Reynolds number directly correlates with the cylinder's surface temperature, the Nusselt number and surface temperature also directly correlate.

The average Nusselt number and average Reynolds numbers for average flow rates in the range $154.34 \leq Re_D \leq 212.51$ are also calculated, as shown in Figure 5.4 with the equation NuD,NL = 0.0214ReD + 8.2517. The quasi-linear relationship had a regression factor of $R^2 = 0.9361$, and this curve was extracted for the middle cylinder to compare it with the side cylinders later.

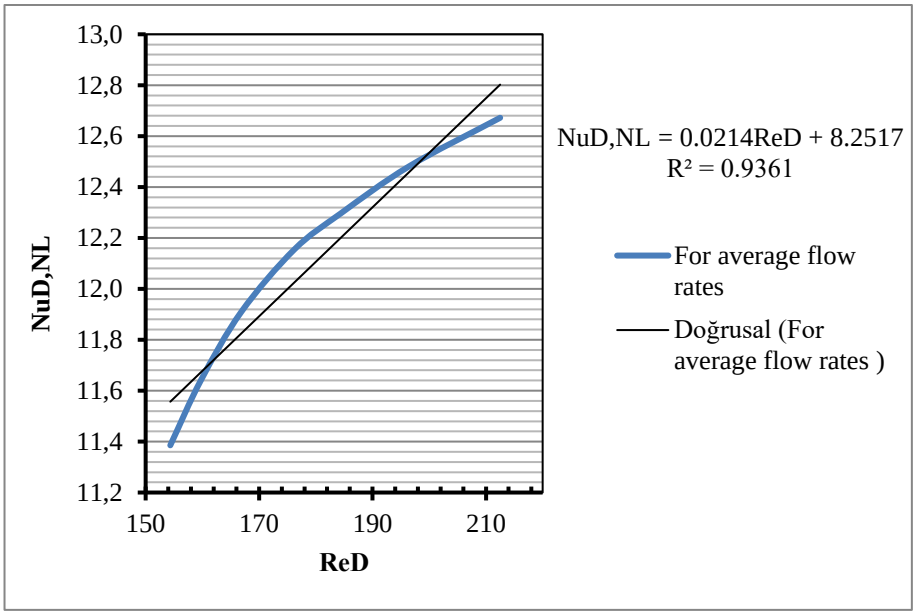

Figure 5.4. Average Nusselt number and average Reynolds numbers for average flow rates for the middle cylinder in an assembly.

5.2. SIDE VERTICAL THIN CYLINDERS IN WATER IN ASSEMBLY-INDUCED CONVECTIVE HEAT TRANSFER

The remaining measurements for the side cylinders are shown in the following figures. Because of the nearly identical outcomes, the values for the two side cylinders were normalized to the same value.

Surface temperature increases when heat flux values increase on the side cylinders, as shown in Figure 5.5, and they are very similar to those obtained for the central cylinder but with lower surface temperatures (the reason for the difference is discussed below).

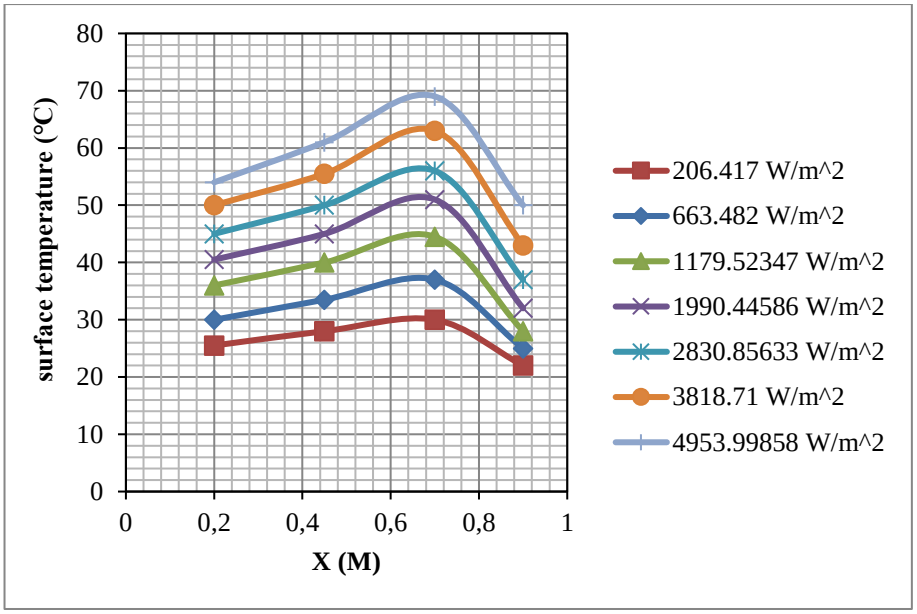

(a)

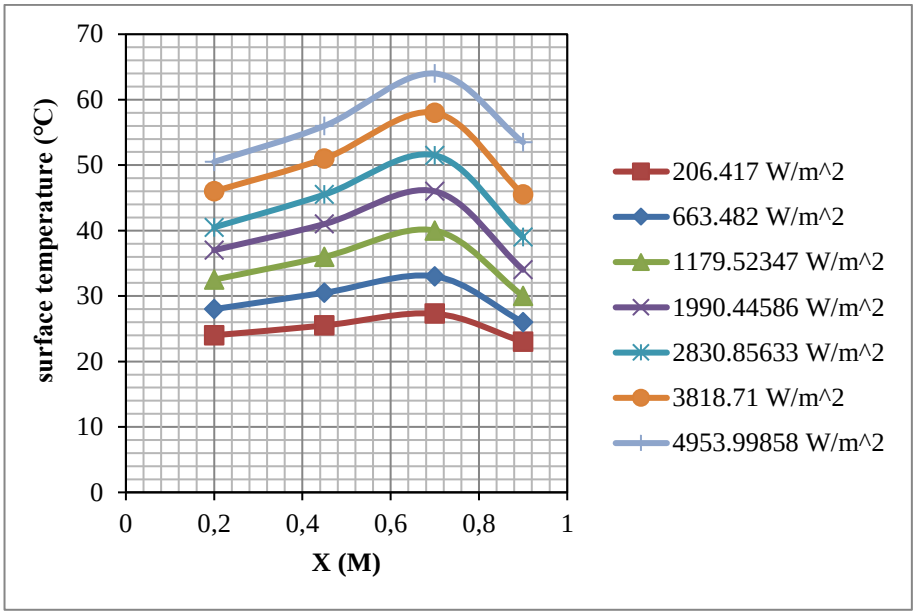

(b)

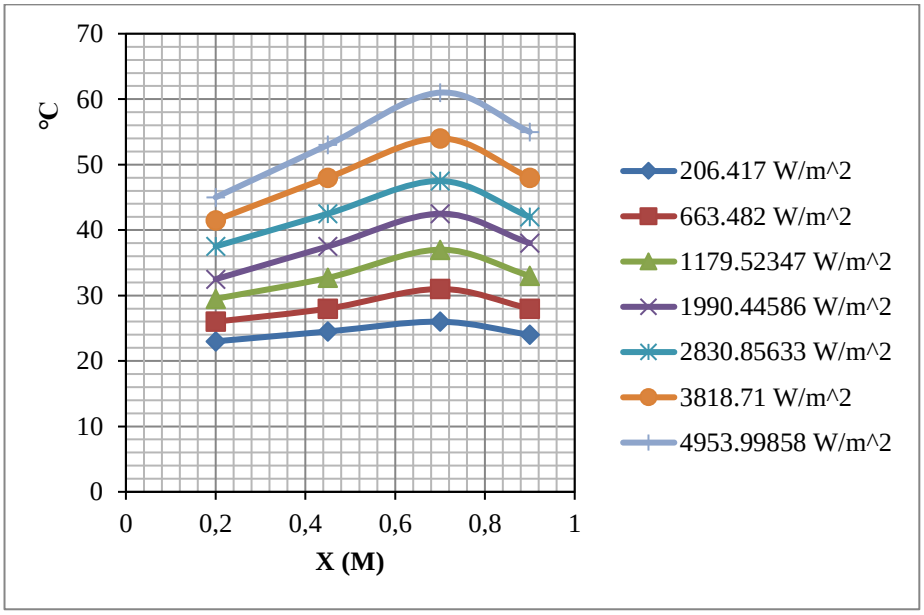

(c)

Figure 5.5. Surface temperatures at three axial positions and in the outlets of the side cylinders in assembly at different uniform heat flux values and flow rates of (a) 32.5 L/M, (b) 25 L/M, and (c) 15.6 L/M.

The surface temperature of the cylinder continues to increase up the axial path, as shown in Figures 5.1 and 5.5. However, the water temperature begins to decrease as it approaches the outlet. This particular decrease was caused by the turbulence produced when hot and cold water were allowed to leave the system through the

same opening. Since the point of departure for the heating area is situated close to the exit for the boundary layer, there is more turbulence in this boundary layer than there would normally be. Typically, there would be less turbulence in this boundary layer. Because of the difference in density between the boundary layer and the bottom-flowing fluid, the layer of cold water mixes with the fluid flowing from the bottom up. This leads to increased speed and turbulence in the boundary layer of this particular location.

The temperature difference between the side and middle cylinders is due to there being less water flowing around the side cylinders than the water flowing around the middle cylinder. This indicates that the surface temperature of the middle cylinder is higher than the surface temperature of the side cylinders because the relationship of water flow with the heat transfer rate is inverse. This is also because the water flow around the middle cylinder is higher than the flow around the side cylinders, which means that the flow rate and the temperature transfer have an inverse relationship. The surface temperature is greater at 700 millimeters from the base of the cylinder, and it even improves as the length of the cylinder increases. This is because there is a greater flow of heat, which leads to increased spacing. The turbulence that the side cylinders generated in the middle cylinders causes the water to move through the surface of the central cylinder at a higher rate than it moves through the surfaces of the other cylinders, as seen in Figures 5.1 and 5.5. The presence of turbulence draws cold water closer to the wall, forcing hot water to move away from the wall and into the flow, where it combines with the cold water drawn closer to the wall by turbulence. Because of the reduction in the rate of local heat transfer, the surface temperature of the middle cylinder is higher than the surface temperatures of the other cylinders.

On the other hand, there was a noticeable increase in the local heat transfer rate in the side cylinders. This difference in flow is caused by disturbances in the boundary layers, the effect of the side cylinders on the middle cylinder, and a phenomenon known as the chimney effect. The difference in fluid flow rates between the central and side locations is the reason for the difference in the surface temperatures. The turbulence makes the temperature difference between the side and center cylinders more pronounced. Water can flow from the wall of the stainless steel cylinder

through the inlet hole and into the two side cylinders on both sides of the central cylinder. The surface temperatures of the two side cylinders will drop slightly due to the increasing rate at which water is circulated through the system.

5.2.1. Correlatıons

It is possible to perform experimental correlations between side cylinders and dimensionless universal numbers to determine how heat moves through an assembly. It is shown in Figure 5.6 that the average Nusselt numbers correspond to the average Reynolds numbers that are appropriate for the various flow rates. The dimensionless correlation between the average Nusselt number and the average Reynolds number is calculated for each flow rate, as shown in Figure 5.6.

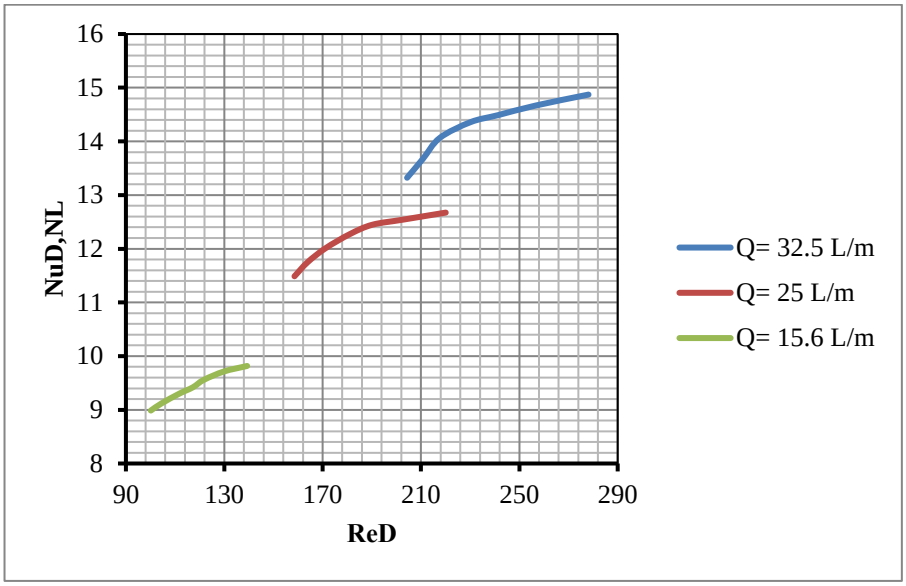

Figure 5.6. Average Nusselt and Reynolds numbers at different heat fluxes at different flow rates for side cylinders in an assembly.

The average Nusselt number and average Reynolds numbers for average flow rates in the range $154.34 \leq Re_D \leq 212.51$ are also extracted, as shown in Figure 5.7, with the equation NuD,NL = 0.0198ReD + 8.3956. The quasi-linear relationship has a regression factor of $R^2 = 0.9106$. This curve was extracted for the side cylinders to compare later with the middle cylinder.

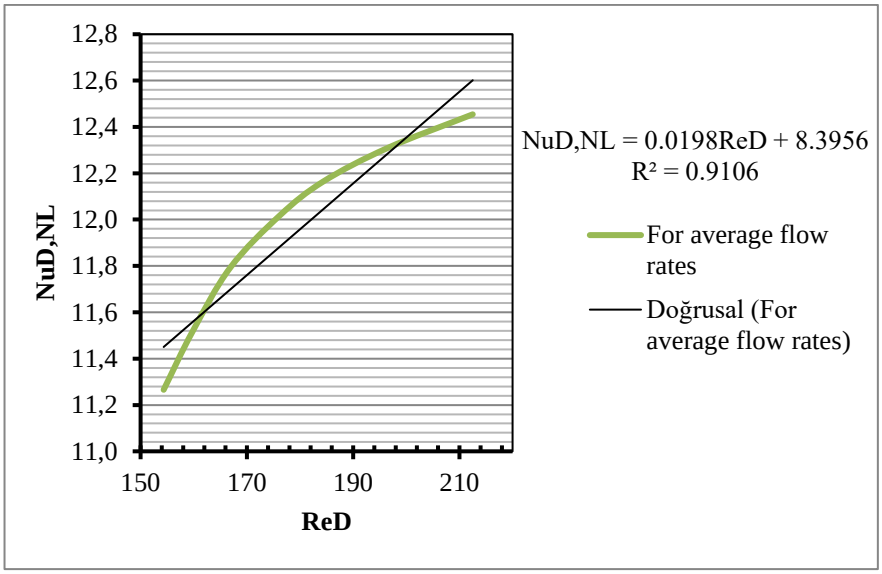

Figure 5.7. Average Nusselt and Reynolds numbers for average flow rates for side cylinders in an assembly.

The average Nusselt number for flow rates tends to rise with the average Reynolds number when the former increases. It is observed that when the flow rate is reduced, the surface temperatures of the cylinders are lower while the water temperature is higher. This is due to improving the increase in heat transfer processes between the cylinder surfaces and the water as the flow rate decreases. The cylinders lose a great amount of heat to the water when the water is moving slowly. The surface temperatures of cylinders in the current study are higher than that of the previous research, as in Figure 5.2, because the previous study was working on natural heat transfer, so they did not use a fluid flow pump. A complete Nusselt number profile would differ for the middle and side cylinders. As previously mentioned, this discrepancy arises from the expanding turbulence in the region created by the heated cylinders. Because the quantity *ReD* is defined by the viscosity of the water, which is determined by the mean temperature of water at intake and exit, as well as the fluid flow rate, there is no difference in the range of *ReD* between various cylinders.

5.3. COMPARISON BETWEEN THE MIDDLE CYLINDER AND THE SIDE CYLINDERS IN THE FINAL RESULTS

The average Nusselt number for average flow rates is depicted here, along with its relationship to the average Reynolds numbers for average flow rates for all cylinders in Figure 5.8. It has been discovered that the side cylinders are the most significant component in terms of heat transport. The average Reynolds numbers for average flow rates range over $154.34 \leq Re_D \leq 212.51$. It can also be seen in Figure 5.8 that the curve deduced two equations, the first being NuD,NL = 0.0214ReD + 8.2517 for the semi-linear relationship for the middle cylinder, which has a regression factor of $R^2 = 0.9361$, and the second being NuD,NL = 0.0198ReD + 8.3956 for the semi-linear relationship for the side cylinders, which has a regression factor of $R^2 = 0.9106$.

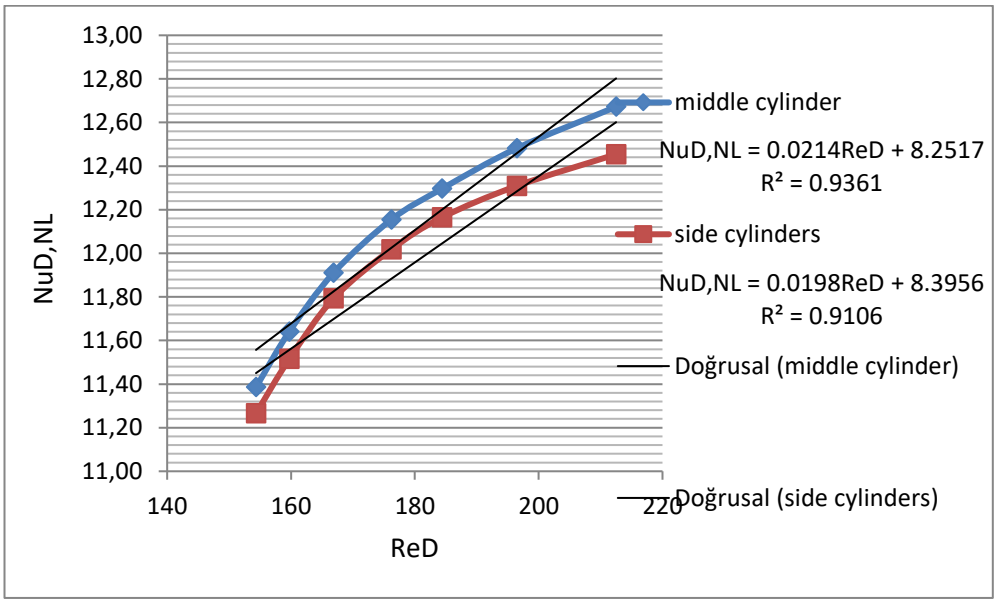

Figure 5.8. Comparison of the average flow rates for all cylinders in terms of average Nusselt and Reynolds numbers in the assembly.

As shown in Figure 5.8, the average Nusselt number for the average flow rates of the middle cylinder has a value higher than the average Nusselt number for the average flow rates of the side cylinders. This is because the water surrounding the central cylinder rises faster than the water surrounding the side cylinders. This causes changes in the physical properties of the water due to the chimney effect.

5.4. STUDY OF THE PUMPING POWER OF THE THREE FLOW RATES

As mentioned earlier, this study used three values for liquid flow rates (32.5 L/M, 25 L/M and 15.6 L/M). The flow rate was converted into a volume flow rate, and the values were compensated by Eq. 3.17 and Eq. 3.18 using the Excel program to produce the graph in Figure 5.9, which shows the relationship between the pumping power and the volume flow rate. It is clear that the relationship with equation $\dot{W}_p = 1.5279\dot{V} - 0.0004$ is semi-linear and has a regression factor of $R^2 = 0.963$. The pumping power range was $0.54 \times 10^{-4} \leq \dot{W}_p \leq 4.9 \times 10^{-4}$.

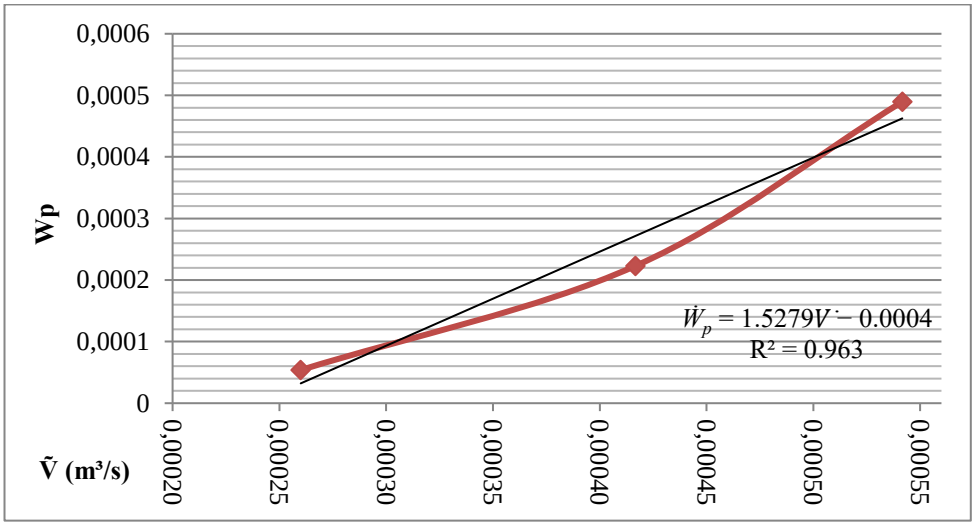

Figure 5.9. The pumping power for each volume flow rate.

PART 6

CONCLUSION

An experimental test of forced convection heat transfer involved using nine thin vertical cylinders immersed in water. Three of these cylinders were heated. The heat flux values and flow rates were modified and the Reynolds numbers were altered. From the present study, it was concluded that, regardless of the heat fluxes used, the overall contour of the surface temperature distribution across the axial distance of the cylinders would remain constant. Furthermore, the water on the surface became heated proportionally with an increasing axial distance of up to 700 mm. At this point, it would begin to decrease due to the turbulent mixing of cold and hot water flowing from the hot cylinders and the turbulence forming from the cold water itself. Along the axial length of the cylinders, a decrease was observed in the heat transfer coefficient due to the increased turbulence present in the boundary layer. It was also discovered that there is a direct relationship between the flow rate of the liquid and the Reynolds and Nusselt numbers, but their relationship is inverse to the water temperature. The results of the cylinder tests were similar to the results obtained from the previous tests. Nusselt and Reynolds numbers can be correlated using empirical correlations for a given flow rate. When the flow rate changes, these connections are in place. The percentage of heat transfer through radiation was approximately three percent at the system's highest energy and highest temperature recorded and thus was ignored. It was also concluded that there is a quasi-linear relationship between the Nusselt number and the Reynolds number, where the following equation extracted the relationship:

$$(Nu_D = \frac{h\,D}{K_f} = ((0.52\,Re_D{}^{0.5}\,Pr^{0.36}\,(\,Pr\,/\,Pr_s\,)^{0.25}) * 0.86)$$

Moreover, a quasi-linear relationship between pumping power and pressure drop was discovered from the equation $W = V \Delta P$. The range of average Reynolds numbers for average flow rates for all heated cylinders was $154.34 \leq Re_D \leq 212.51$, and the range

of pumping power was $0.54 \times 10^{-4} \leq \dot{W}_p \leq 4.9 \times 10^{-4}$. During the testing, the heat flux values were held at 14.75 W/m^2, 206.417 W/m^2, 663.482 W/m^2, 1,179.52347 W/m^2, 1,990.44586 W/m^2, 2,830.85633 W/m^2, 3,818.71 W/m^2, and 4,953.99858 W/m^2. However, the first value (14.75 W/m^2) was minimal and was therefore not taken into account and disregarded. The following are the most important discoveries through the experimental tests and the application of equations:

1. The effect of the water on the heat transfer rate from the surface of the heated cylinders decreases when the water flow velocity is raised.
2. When the water flow rate increases, the water temperature decreases while the surface temperature of the heated cylinders increases.
3. The surface temperature of the heated cylinders is higher in forced convection compared to natural convection because there is water flow in the forced convection.
4. The average Nusselt number increases as the water flow rate increases.
5. The dimensionless numbers, the average Nusselt number, and the average Reynolds number have a direct relationship, while their relationship is positive with the surface temperature of the heated cylinders.
6. The side-heated cylinders lose more heat than the heated cylinder placed in the middle of the group because the side-heated cylinders affect the speed of water flow in the middle of the group and because of the chimney effect.

6.1. RECOMMENDATIONS

1. Heating the remaining cylinder using the same cylinder with the same dimensions.
2. Visualizing laminar and turbulent zones with a high-definition thermal camera.
3. Adjusting the distances between the centers of two cylinders to the diameter ratio (S_T/D) and power.
4. Using higher Reynolds numbers of up to 250.
5. Using other bulk fluids, such as oil.
6. Using a more powerful pump of a different type.

7. Increasing the heat flux.
8. Conducting the experiment horizontally.

REFERENCES

1. Mansir, I.B., Ben-Mansour, R., and Habib, M.A., "Numerical modeling of heat transfer characteristics in a two-pass oxygen transport reactor for fire tube boilers under oxy-fuel combustion", ***Appl. Therm. Eng.***, 195: (2021).

2. Bhattacharya, S., Verma, M.K., and Samtaney, R., "Revisiting Reynolds and Nusselt numbers in turbulent thermal convection", ***Phys. Fluids***, 33 (1): (2021).

3. Wei, Y., Liu, X., Zhu, K., and Huang, Y., "A unified lattice Boltzmann framework for combined radiation-conduction heat transfer", ***Int. J. Heat Mass Transf.***, 200: 123513 (2023).

4. Verma, S., Freeman, B.R.S., and Hemmati, A., "Effects of Reynolds number and average angle of attack on the laminar scaling of oscillating foils", ***Phys. Fluids***, 34 (3): 31905 (2022).

5. Vučetić, N., Jovičić, G., Antunović, R., Sovilj-Nikić, S., Košarac, A., and Jeremić, D., "INTEGRITY ASSESSMENT OF AN AIRCRAFT CYLINDER ASSEMBLY WITH A CRACK", ***Mater. Tehnol.***, 56 (4): (2022).

6. Huang, B., Zhao, Q., Sun, C., Zhu, L., Zhang, H., Zhang, Y., Liu, C., and Li, F., "Trace Analysis of Gases and Liquids with Spontaneous Raman Scattering Based on the Integrating Sphere Principle", ***Anal. Chem.***, (2022).

7. Internet: BYJU'S, "What Is Convection? - Heat Definition, Types of Convection, Examples, Video and FAQs", **https://byjus.com/physics/heat-transfer-convection** 2022.

8. Talmor, M. and Seyed-Yagoobi, J., "Electrohydrodynamically Augmented Internal Forced Convection", Handb. Therm. Sci. Eng., ***Springer International Publishing***, Cham, 479–526 (2018).

9. Wang, Z.H. and Zhou, Z.K., "External natural convection heat transfer of liquid metal under the influence of the magnetic field", ***Int. J. Heat Mass Transf.***, 134: 175–184 (2019).

10. Han, J.-C. and Wright, L.M., "External Forced Convection", Anal. Heat Transf., ***CRC Press***, Boca Raton, 203–265 (2022).

11. Cavazzuti, M., "A Forced Convection Application: Surface Optimization for Enhanced Heat Transfer", Optim. Methods, ***Springer Berlin Heidelberg***, Berlin, Heidelberg, 153–173 (2013).

12. Chaudhry, M.H., “GOVERNING EQUATIONS FOR ONE-DIMENSIONAL FLOW”, Open-Channel Flow, ***Springer International Publishing***, Cham, 347–362 (2022).

13. Irfansah, R., Lubis, A., Ansyori, A., and R, T.O., “RANCANG BANGUN ALAT PENGERING CABAI SISTEM TUBULAR HEATER DENGAN MEMANFAATKAN ENERGI SURYA”, ***Prosiding SENAPENMAS***, 1413 (2021).

14. Xia, T., Han, Y., Zhu, C., Sun, Z., Yuan, C., Cui, Q., Cheng, J.-G., Du, W., Li, W., Xie, K., Huang, K., Feng, S., Walker, D., and Li, M.-R., “Thermochemical Mechanism of Optimized Lanthanum Chromite Heaters for High-Pressure and High-Temperature Experiments”, ***ACS Appl. Mater. Interfaces***, 14 (28): 32244–32252 (2022).

15. Storrs Hall, J., “VARIAC: An autogenous cognitive architecture”, ***Front. Artif. Intell. Appl.***, 171 (1): 176–187 (2008).

16. Adepoju, A.T. and Oluwafisoye, P.A., “DEVELOPMENT AND IMPLEMENTATION OF A CONTROLLER FOR 220 VOLTS, 2.5 HORSEPOWER LIQUID PUMP”, 6: 113–117 (2019).

17. Sunil Shivaji, D. and Sumit, D.S., “Stress Analysis of Gate Valve By Ansys”, ***DAV Int. J. Sci.***, (May): 2014 (2014).

18. Seban, R.A. and Drake, R.M., “Local Heat-Transfer Coefficients on the Surface of an Elliptical Cylinder in a High-Speed Air Stream”, ***J. Fluids Eng.***, 75 (2): 235–239 (1953).

19. Drake, R.M., Seban, R.A., Doughty, D.L., and Levy, S., “Local Heat-Transfer Coefficients on Surface of an Elliptical Cylinder, Axis Ratio 1:3, in a High-Speed Air Stream”, ***J. Fluids Eng.***, 75 (7): 1291–1301 (1953).

20. Khosla, J., Hoffman, T.W., and Pollock, K.G., “Combined Forced and Natural Convective Heat Transfer To Air in a Vertical Tube.”, 144–148 (1974).

21. Ota, T., Aiba, S., Tsuruta, T., and Kaga, M., “Forced Convection Heat Transfer From an Elliptic Cylinder of Axis Ratio 1:2.”, ***Bull. JSME***, 26 (212): 262–267 (1983).

22. Ota, T., Nishiyama, H., and Taoka, Y., “Heat transfer and flow around an elliptic cylinder”, ***Int. J. Heat Mass Transf.***, 1771–1779 (1984).

23. Nishiyama, H., Ota, T., and Matsuno, T., “Forced Convection Heat Transfer From Two Elliptic Cylinders in a Tandem Arrangement.”, ***Heat Transf. - Japanese Res.***, 17 (3): 19–31 (1988).

24. Merker, G.P. and Hanke, H., “Experimental results of heat transfer and pressure drop on the shell-side of compact cross-flow tubular heat exchangers.”, ***Int. J. Heat Mass Transf.***, 1903–1909 (1986).

25. Ilgarubis, V.A.S., Ulinskas, R.V, and Butkus, A.V, "Hydraulic Drag and Average Heat Transfer Coefficients of Compact Bundles of Elliptical Finned Tubes.", ***Heat Transf. Sov. Res.***, 20 (1): 12–21 (1988).

26. Prasad, B.V.S.S.S., Tawfek, A.A., and Rao, V.R.M., "Heat transfer from aerofoils in cross-flow", ***Int. Commun. Heat Mass Transf.***, 19 (6): 879–890 (1992).

27. Badr, H.M., "Laminar natural convection from an elliptic tube with different orientations", ***J. Heat Transfer***, 119 (4): 709–718 (1997).

28. Badr, H.M. and Shamsher, K., "Free convection from an elliptic cylinder with major axis vertical", ***Int. J. Heat Mass Transf.***, 36 (14): 3593–3602 (1993).

29. Rocha, L.A.O., Saboya, F.E.M., and Vargas, J.V.C., "A comparative study of elliptical and circular sections in one- and two-row tubes and plate fin heat exchangers", ***Int. J. Heat Fluid Flow***, 18 (2): 247–252 (1997).

30. Badr, H.M., "Forced convection from a straight elliptical tube", ***Heat And Mass Transfer/Waerme- Und Stoffuebertragung***, 34 (2–3): 229–236 (1998).

31. Bordalo, S.N. and Saboya, F.E.M., "Pressure drop coefficients for elliptic and circular sections in one, two and three-row arrangements of plate fin and tube heat exchangers", ***Rev. Bras. Ciencias Mec. Brazilian Soc. Mech. Sci.***, 21 (4): 600–610 (1999).

32. Castiglia, D., Balabani, S., Papadakis, G., and Yianneskis, M., "An experimental and numerical study of the flow past elliptic cylinder arrays", ***Proc. Inst. Mech. Eng. Part C J. Mech. Eng. Sci.***, 215 (11): 1287–1302 (2001).

33. Badr, H.M., Dennis, S.C.R., and Kocabiyik, S., "Numerical simulation of the unsteady flow over an elliptic cylinder at different orientations", ***Int. J. Numer. Methods Fluids***, 37 (8): 905–931 (2001).

34. Hasan, A. and Sirén, K., "Performance investigation of plain circular and oval tube evaporatively cooled heat exchangers", ***Appl. Therm. Eng.***, 24 (5–6): 777–790 (2004).

35. Tiwari, S., Maurya, D., Biswas, G., and Eswaran, V., "Heat transfer enhancement in cross-flow heat exchangers using oval tubes and multiple delta winglets", ***Int. J. Heat Mass Transf.***, 46 (15): 2841–2856 (2003).

36. Matos, R.S., Laursen, T.A., Vargas, J.V.C., and Bejan, A., "Three-dimensional optimization of staggered finned circular and elliptic tubes in forced convection", ***Int. J. Therm. Sci.***, 43 (5): 477–487 (2004).

37. Bouris, D., Konstantinidis, E., Balabani, S., Castiglia, D., and Bergeles, G., "Design of a novel, intensified heat exchanger for reduced fouling rates", ***Int. J. Heat Mass Transf.***, 48 (18): 3817–3832 (2005).

38. Yamazaki, S.A. and Y., "Three Cylinders", ***J. Heat Transfer***, 503–508 (1976).

39. Kinebuchi, T. and Shimamoto, N., “One-dimensional diffusion of TrpR along DNA enhances its affinity for the operator by chemical ratchet mechanism”, ***Sci. Rep.***, 11 (1): 4255 (2021).

40. ŽUKAUSKAS, A. and ULINSKAS, R., “Efficiency Parameters for Heat Transfer in Tube Banks”, ***Heat Transf. Eng.***, 6 (1): 19–25 (1985).

41. Zdravkovich, M.M., “The effects of interference between circular cylinders in cross flow”, ***J. Fluids Struct.***, 1 (2): 239–261 (1987).

42. Horvat, A., Leskovar, M., and Mavko, B., “Comparison of heat transfer conditions in tube bundle cross-flow for different tube shapes”, ***Int. J. Heat Mass Transf.***, 49 (5–6): 1027–1038 (2006).

43. Nouri-Borujerdi, A. and Lavasani, A., “Flow measurement around a non-circular tube”, ***5th Int. Conf. Heat Transf.***, (2007).

44. Ibrahim, T.A. and Gomaa, A., “Thermal performance criteria of elliptic tube bundle in crossflow”, ***Int. J. Therm. Sci.***, 48 (11): 2148–2158 (2009).

45. Janjua, M.M., Khan, N.U., Khan, W.A., Khan, W.S., and Ali, H.M., “Numerical study of forced convection heat transfer across a cylinder with various cross sections”, ***J. Therm. Anal. Calorim.***, 143 (3): 2039–2052 (2021).

46. Atkinson, K. and Han, W., “Theoretical Numerical Analysis”, Texts Appl. Math., (2001).

47. Choudhury, A., Routray, D., Swain, S., and Das, A.K., “Prevalence and risk factors of people at-risk of obstructive sleep apnea in a rural community of Odisha, India: a community based cross-sectional study”, ***Sleep Med.***, 58: 42–47 (2019).

48. Sayed Ahmed, S.A.E., Mesalhy, O.M., and Abdelatief, M.A., “Flow and heat transfer enhancement in tube heat exchangers”, ***Heat Mass Transf.***, 51 (11): 1607–1630 (2015).

49. Bayat, H., Lavasani, A.M., Bolhasani, M., and Moosavi, S., “Numerical Study of Flow around Flat Tube between Parallel Walls”, 8 (8): 1468–1471 (2014).

50. Mir, A., Lavasani, A., and Bayat, H., “Heat Transfer from Two Cam Shaped Cylinders in Side-by-Side Arrangement”, 6 (2): 1008–1011 (2012).

51. Zhang, H., Sun, Q., Sun, Z., and Lu, Y., “Experimental and Numerical Investigation of Electromigration Behavior of Printed Silver Wire Under High Current Density”, ***J. Electron. Packag.***, 145 (2): (2023).

52. Zhang, H.-F. and Lavan, Z., “Thermal performance of a serpentine absorber plate”, ***Sol. Energy***, 34 (2): 175–177 (1985).

53. Sahim, K. and Puspitasari, D., “Convective heat transfer of one row arrangement of elliptical cylinder”, ***Front. Heat Mass Transf.***, 8: (2017).

54. Chen, L.G., Li, Y.S., and Wong, K.K., “An efficient semi-implicit finite element scheme for two-dimensional tidal flow computations”, ***Comput. Mech.***, 5 (2–3): 161–173 (1989).

55. Lavasani, A.M., Maarefdoost, T., and Bayat, H., “Effect of blockage ratio on pressure drag and heat transfer of a cam-shaped tube”, ***Heat Mass Transf.***, 52 (9): 1935–1942 (2016).

56. Deepakkumar, R., Jayavel, S., and Tiwari, S., “Cross Flow past Circular Cylinder with Waviness in Confining Walls near the Cylinder”, ***J. Appl. Fluid Mech.***, 10 (1): 183–197 (2017).

57. Gholami, A.A., Wahid, M.A., and Mohammed, H.A., “Heat transfer enhancement and pressure drop for fin-and-tube compact heat exchangers with wavy rectangular winglet-type vortex generators”, ***Int. Commun. Heat Mass Transf.***, 54: 132–140 (2014).

58. Mangrulkar, C.K., Abraham, J.D., and Dhoble, A.S., “Numerical studies on the near wall y + effect on heat and flow characteristics of the cross flow tube bank”, ***J. Phys. Conf. Ser.***, 1240 (1): 12110 (2019).

59. Mangrulkar, C.K., Dhoble, A.S., Pant, P.K., Kumar, N., Gupta, A., and Chamoli, S., “Thermal performance escalation of cross flow heat exchanger using in-line elliptical tubes”, ***Exp. Heat Transf.***, 33 (7): 587–612 (2020).

60. Mohanty, R.L., Swain, A., and Das, M.K., “Thermal performance of mixed tube bundle composed of circular and elliptical tubes”, ***Therm. Sci. Eng. Prog.***, 5: 492–505 (2018).

61. Khalifa, A.J.N. and Hussien, Z.A., “Natural convection heat transfer from a single and multiple heated thin cylinders in water”, ***Heat Mass Transf.***, 51 (11): 1579–1586 (2015).

62. Cengel, Y.A., “Heat and Mass Transfer FUNDANMENTAL & APPLICATIONS”, ***News.Ge***, 1057 (2020).

63. Holman, J.P., “Heat Transfer”, 10th Ed. Ed.,

64. Çengel, Y.A. and Ghajar, A.J. (Afshin J., “Heat and mass transfer : fundamentals & applications”, 1018.

APPENDIX A

Properties of water (saturated liquid)

°F	°C	c_p kJ/kg · °C	ρ kg/m^3	μ kg/m · s	k W/m · °C	Pr
32	0	4.225	999.8	1.79×10^{-3}	0.566	13.25
40	4.44	4.208	999.8	1.55	0.575	11.35
50	10	4.195	999.2	1.31	0.585	9.40
60	15.56	4.186	998.6	1.12	0.595	7.88
70	21.11	4.179	997.4	9.8×10^{-4}	0.604	6.78
80	26.67	4.179	995.8	8.6	0.614	5.85
90	32.22	4.174	994.9	7.65	0.623	5.12
100	37.78	4.174	993.0	6.82	0.630	4.53
110	43.33	4.174	990.6	6.16	0.637	4.04
120	48.89	4.174	988.8	5.62	0.644	3.64
130	54.44	4.179	985.7	5.13	0.649	3.30
140	60	4.179	983.3	4.71	0.654	3.01
150	65.55	4.183	980.3	4.3	0.659	2.73
160	71.11	4.186	977.3	4.01	0.665	2.53
170	76.67	4.191	973.7	3.72	0.668	2.33
180	82.22	4.195	970.2	3.47	0.673	2.16
190	87.78	4.199	966.7	3.27	0.675	2.03
200	93.33	4.204	963.2	3.06	0.678	1.90
220	104.4	4.216	955.1	2.67	0.684	1.66
240	115.6	4.229	946.7	2.44	0.685	1.51
260	126.7	4.250	937.2	2.19	0.685	1.36
280	137.8	4.271	928.1	1.98	0.685	1.24
300	148.9	4.296	918.0	1.86	0.684	1.17
350	176.7	4.371	890.4	1.57	0.677	1.02
400	204.4	4.467	859.4	1.36	0.665	1.00
450	232.2	4.585	825.7	1.20	0.646	0.85
500	260	4.731	785.2	1.07	0.616	0.83
550	287.7	5.024	735.5	9.51×10^{-5}		
600	315.6	5.703	678.7	8.68		

Properties of water (saturated liquid) [63].

APPENDIX B

Charts and tables used in equations

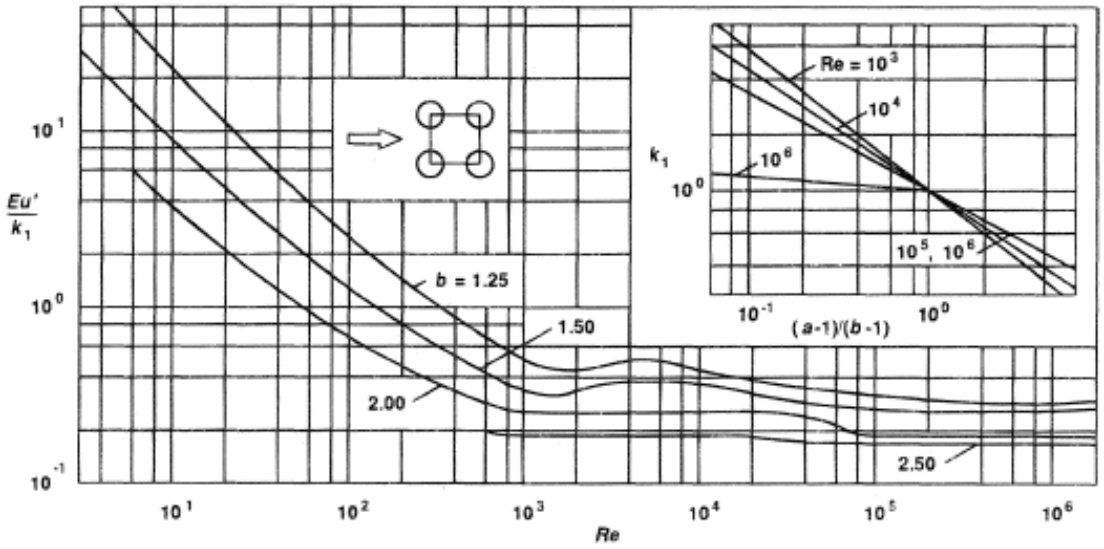

Friction factor f and correction factor X for tube banks [64][62].

Arrangement	Range of Re_D	Correlation
In-line	0–100	$Nu_D = 0.9\ Re_D^{0.4} Pr^{0.36} (Pr/Pr_s)^{0.25}$
	100–1000	$Nu_D = 0.52\ Re_D^{0.5} Pr^{0.36} (Pr/Pr_s)^{0.25}$
	1000–2×10^5	$Nu_D = 0.27\ Re_D^{0.63} Pr^{0.36} (Pr/Pr_s)^{0.25}$
	2×10^5–2×10^6	$Nu_D = 0.033\ Re_D^{0.8} Pr^{0.4} (Pr/Pr_s)^{0.25}$
Staggered	0–500	$Nu_D = 1.04\ Re_D^{0.4} Pr^{0.36} (Pr/Pr_s)^{0.25}$
	500–1000	$Nu_D = 0.71\ Re_D^{0.5} Pr^{0.36} (Pr/Pr_s)^{0.25}$
	1000–2×10^5	$Nu_D = 0.35(S_T/S_L)^{0.2}\ Re_D^{0.6} Pr^{0.36} (Pr/Pr_s)^{0.25}$
	2×10^5–2×10^6	$Nu_D = 0.031(S_T/S_L)^{0.2}\ Re_D^{0.8} Pr^{0.36} (Pr/Pr_s)^{0.25}$

Nusselt number correlations for cross flow over tube banks for NL > 16 and 0.7 < Pr < 500 [64][62].

N_L	1	2	3	4	5	7	10	13
In-line	0.70	0.80	0.86	0.90	0.93	0.96	0.98	0.99
Staggered	0.64	0.76	0.84	0.89	0.93	0.96	0.98	0.99

Correction factor F to be used in $Nu_{D,NL} = F\ Nu_D$ for NL < 16 [64][62].

APPENDIX C

SAMPLE OF ERROR CALCULATION

As an example, the following case (in the case of the highest power and highest temperatures recorded) is presented:

Total power = 840 W, $\overline{T}_{s_L} = 66.66667℃$, $T_m = 42$ ℃ and
$A_S = N\pi DL$ ... A_s 0.16956 m^2.

Computation of the radiation heat transfer

σ = Stefan-Boltzmann constant = 5.669 × 10^{-8} W/m² K^4, ε = 0.85 (emissivity of stainless steel).

$$Q_{rad} = \varepsilon A_s \sigma (T_s^4 - T_m^4)$$

$$Q_{rad} = 0.85 \times 0.169\,56 \times 5.669 \times 10^{-8} ((66.66667 + 273)^4 - (42 + 273)^4$$

$$Q_{rad} = 28.31432\ W$$

Computation of the convection heat transfer

The total heat transfer is calculated from:

$$Q = Q_{cond} = Q_{conv} + Q_{rad}$$

Convection heat transfer is calculated from the above equation, and by disregarding the conduction heat transfer that was discussed in Part 3:

$$840 = Q_{conv} + 28.31432 \quad \ldots\ldots \quad Q_{conv} = 811.7\ W$$

The rate of heat transfer by radiation is very low compared to the rate of heat transfer by convection. When ignoring radiation heat transfer, the maximum error is:

$Error = \frac{840\ W - 811.7W}{840\ W} \times 100 = 3.37\%$ for all heated cylinders.

CURRICULUM VITAE

Ibrahim Amer Mahmoud is a mechanical engineer who graduated from the Faculty of Engineering, University of Dijlah, Iraq. He received his Bachelor's degree in 2019. He is currently studying for his Master degree at Karabük University in the field of Mechanical Engineering.